Carbohydrate Polymers 291 (2022) 119655

Contents lists available at ScienceDirect

Carbohydrate Polymers

journal homepage: www.elsevier.com/locate/carbpol

Polysaccharides from *Aconitum carmichaelii* leaves: Structure, immunomodulatory and anti-inflammatory activities

Yu-Ping Fu [a,*], Cen-Yu Li [b], Xi Peng [b], Yuan-Feng Zou [b], Frode Rise [c], Berit Smestad Paulsen [a], Helle Wangensteen [a], Kari Tvete Inngjerdingen [a]

[a] Section for Pharmaceutical Chemistry, Department of Pharmacy, University of Oslo, P.O. Box 1068, Blindern, 0316 Oslo, Norway
[b] Natural Medicine Research Center, College of Veterinary Medicine, Sichuan Agricultural University, 611130 Wenjiang, PR China
[c] Department of Chemistry, University of Oslo, P.O. Box 1033, Blindern, 0315 Oslo, Norway

ARTICLE INFO

Keywords:
Aconitum carmichaelii leaves
Pectin
Hemicellulose
Complement fixation activity
Intestinal anti-inflammatory activity

ABSTRACT

Roots of *Aconitum carmichaelii* are used in Asian countries due to its content of bioactive alkaloids. In the production of root preparations, tons of leaves are usually discarded, leading to a huge waste of herbal material. The aim of this study is to investigate the polysaccharides in these unutilized leaves. A neutral polysaccharide (AL-N) appeared to be a mixture of heteromannans, and two purified acidic polysaccharides (AL-I-I and AL-I-II) were shown to be pectins containing a homogalacturonan backbone substituted with terminal β-Xyl*p*-units. AL-I-I consisted of a type-I rhamnogalacturonan core, with arabinan and type-II arabinogalactan domains while AL-I-II was less branched. AL-N and AL-I-I were able to modulate the complement system, while AL-I-II was inactive. Interestingly, AL-N, AL-I-I and AL-I-II were shown to exert anti-inflammatory effects on porcine enterocyte IPEC-J2 cells. AL-I-I and AL-I-II were able to down-regulate the expression of toll-like receptor 4 (TLR4) and nucleotide-binding oligomerization domain 1 (NOD1).

1. Introduction

Aconitum carmichaelii Debeaux (Ranunculaceae) is indigenous mainly to China, but can be found in other Asian countries, and also in Europe (Fu et al., 2022). It is a perennial herb, 60–150 cm high, with pentagonal leaves 6–11 cm long and 9–15 cm wide (Committee for the flora of China, 2004). In China, the lateral and mother roots of *A. carmichaelii*, known as "Fuzi" and "Chuanwu", are used in Traditional Chinese Medicine (TCM) in the treatment of acute myocardial infarction, rheumatoid arthritis, and coronary heart disease, as well as for analgesic use (Chinese Pharmacopoeia Committee, 2020; Fu et al., 2022). Currently, the plant is commercially grown in Sichuan Province, where most of the trading of "Fuzi" and "Chuanwu" exist. More than 200 tons of dried roots were traded within the two year period from 2015 to 2017 (China Academy of Chinese Medical Science, 2017).

The market of TCM is attractive, but a great amount of unutilized parts of medicinal plants is generated from the industry, such as stems and leaves for TCM based on roots. A better utilization of bio-resources is highly required, and these residues should be recycled and converted into valuable products such as phytochemicals (Huang, Li, et al., 2021; Huang, Peng, et al., 2021; Saha & Basak, 2020). The aerial parts of *A. carmichaelii*, making up 40% of the biomass of the whole plant, are normally discarded after the roots are harvested, and a vast amount of waste of this plant source is consequently generated. To date, the aerial parts of *A. carmichaelii* have shown similar analgesic and anti-inflammatory activities as for the roots (He et al., 2018). Alkaloids, flavonoids, lignin (Duc et al., 2015; Zhang, Yang, et al., 2020), fatty acids (Chen, 2011; Ni et al., 2002), sterols (Guo, 2012; Yang et al., 2011) and polysaccharides (Ou et al., 2013) have been identified in the leaves. A content of approximately 5% (on dry basis) polysaccharides has been determined in *A. carmichaelii* leaves (Ou et al., 2013), but further studies on structural characterization and pharmacology have not been performed.

Many natural polysaccharides are unable to be digested by mammalian enzymes in the gastrointestinal tract, and act as dietary fiber. These have attracted increasing attention due to their positive health effects, such as immunoregulatory, anti-tumor, anti-viral, anti-oxidative, and hypoglycemic activities, and low toxicity (Yang et al., 2022; Yu et al., 2018). Pectins, for instance, have been shown to exert potent immunomodulatory effects on the complement system,

* Corresponding author.
E-mail address: y.p.fu@farmasi.uio.no (Y.-P. Fu).

https://doi.org/10.1016/j.carbpol.2022.119655
Received 4 March 2022; Received in revised form 19 May 2022; Accepted 22 May 2022
Available online 27 May 2022

macrophages, T cells, natural killer cells, and the intestinal immune system (Beukema et al., 2020; Zaitseva et al., 2020). It has been suggested that pectic polysaccharides could interact with plasma complement proteins *via* the alternative and/or the classical pathways. This could lead to either activation of the complement system, which contributes to inflammatory responses in addition to host defense reactions, or inhibition of complement cascade which would be a good therapeutic strategy for treating inflammatory diseases (Yamada & Kiyohara, 2007). Pectins have also attracted growing attention for their role in the preservation of epithelial integrity, and might directly interact with pattern recognition receptors, such as Toll-like receptors 2 (TLR2) and 4 (TLR4) or Galectin-3 (Beukema et al., 2020), inhibit inflammation and oxidative responses, or modulate the levels of cytokines and chemotactic factors (Huang et al., 2017; Tang et al., 2019). Therefore, we hypothesized that the unutilized leaves of *A. carmichaelii* could be a potential medicinal source due to the presence of polysaccharides with possible immunomodulatory and anti-inflammatory activities.

The aim of this study was to isolate and characterize polysaccharides present in the leaves of *A. carmichaelii* and to determine their complement fixation activity and intestinal anti-inflammatory effects on lipopolysaccharide (LPS)-induced inflammatory intestinal epithelial cells (IPEC-J2).

2. Materials and methods

2.1. Materials

The whole plant of *A. carmichaelii* Debeaux was collected in Wudu Village, Jiangyou City, Sichuan Province, P.R. China in June 2019 (31°50′24.0″N/ 104°47′24.0″E, 517.11 m), and was identified by Yuan-Feng Zou, Sichuan Agricultural University. A voucher specimen with number 2019-06-342 is deposited in the Department of Pharmacy, Sichuan Agricultural University. The fresh leaves were separated from the rest of the plant immediately after collection, and then dried in a drying oven at 40 °C with flowing air.

2.2. Isolation and purification of polysaccharides from *A. carmichaelii* leaves

Polysaccharides from *A. carmichaelii* leaves were isolated and purified as depicted in Fig. 1. Fifty grams of dried leaves of *A. carmichaelii* were pre-extracted with 96% ethanol (500 mL, 1 h × 4) under reflux in order to remove small molecular weight and other lipophilic compounds. The dried residues were further extracted with boiling water (1 L, 1 h × 2) under reflux. The combined aqueous extracts were filtered, evaporated at 50 °C, added 4-fold volumes of ethanol and kept at 4 °C for 24 h for precipitation of the polysaccharides. The precipitant was redissolved in distilled water, dialyzed with cut-off 3500 Da, and freeze-dried, giving a crude polysaccharide fraction, named ALP (*A. carmichaelii* Leaves Polysaccharide).

ALP (2.1 g) was fractioned by anion exchange chromatography using a column packed with ANX Sepharose™ 4 Fast Flow (high sub) material (GE Healthcare, 5 × 40 cm). A neutral fraction (AL-N) was first eluted with distilled water (600 mL) with flow rate 1 mL/min, while an acidic fraction (AL-I) was eluted with a linear gradient of NaCl (0–1.5 M, 1200 mL) with flow rate 2 mL/min. 10 mL fractions were collected and

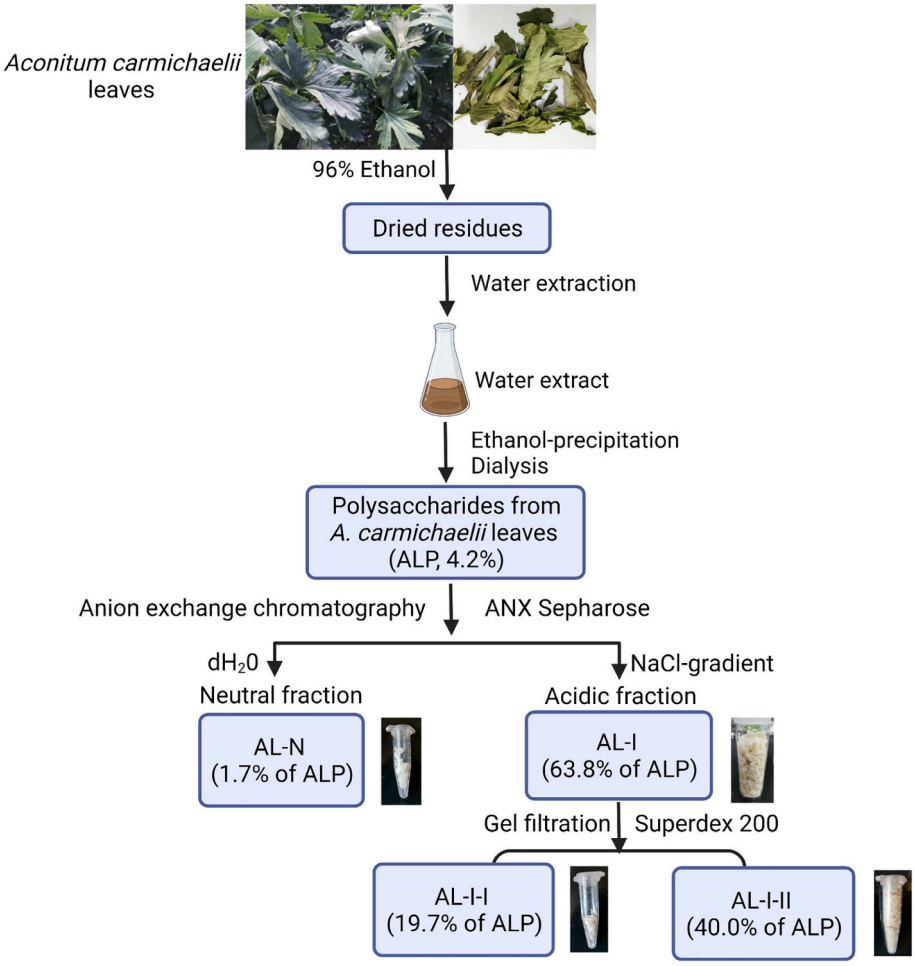

Fig. 1. Work flow of isolation and purification of polysaccharides from *A. carmichaelii* leaves.

monitored by phenol-sulfuric acid assay to locate the polysaccharides (Dubois et al., 1956). The related fractions were combined and dialyzed at cut-off 3500 Da for removal of NaCl, and lyophilized.

AL-I (20 mg) was further separated by size exclusion chromatography (SEC) based on differences in molecular size. 2 mL sample (10 mg/mL in 10 mM NaCl) was applied onto an Hiload™ 16/60 Superdex 200 prep grade column (GE Healthcare) using the Äkta FPLC system (Pharmacia Äkta, Amersham Pharmacia Biotech, Uppsala, Sweden), and eluted with 10 mM NaCl, 0.5 mL/min (2 mL per tube). Fractions were combined based on their elution profiles after phenol-sulfuric acid assay (Dubois et al., 1956), then dialyzed and lyophilized.

2.3. Determination of the chemical composition and monosaccharide composition

The total amounts of phenolic compounds and proteins per fraction were quantitatively determined by Folin-Ciocalteu (Singleton & Rossi, 1965) and Bio-Rad protein assay (Bradford, 1976) respectively. Standard curves were prepared using gallic acid (0–50 μg/mL) for determination of phenolic compounds, and bovine serum albumin for protein determination (BSA, 1.5–25 μg/mL).

The monosaccharide composition of the fractions were determined as described by Chambers and Clamp (1971) with modifications as described before (Wold et al., 2018). In short, samples were subjected to methanolysis using 3 M hydrochloric acid in water-free methanol for 24 h at 80 °C, then trimethylsilylated (TMS) before they were analyzed using capillary gas chromatography (GC) on a Trace™ 1300 GC (Thermo Scientific™, Milan, Italy). Mannitol was used as an internal standard, and calibration curves were prepared by TMS-derived standards, including arabinose (Ara), rhamnose (Rha), fucose (Fuc), xylose (Xyl), mannose (Man), galactose (Gal), glucose (Glc), glucuronic acid (GlcA) and galacturonic acid (GalA). The Chromelion Software v.6.80 (Dionex Corporation, Sunnyvale, CA, USA) was used for GC data analysis.

2.4. Glycosidic linkage determination by methylation and GC/MS

Determination of glycosidic linkages of the different monosaccharides was performed after permethylation of the reduced polymers or native not containing uronic acid. Briefly, 2 mg of samples with uronic acids was reduced to their corresponding neutral sugars with sodium borodeuteride ($NaBD_4$) after activation by carbodiimide, which led to dideuteration in position 6 ($-CD_2-$). This gives an increased mass of related ion fragments ($M^+ + 2$) and helped to distinguish uronic acid from the neutral sugar. Then methylation, hydrolysis, reduction, and acetylation were performed according to previously published methods (Ciucanu & Kerek, 1984; Pettolino et al., 2012; Wold et al., 2018). These derivatives were extracted with dichloromethane, and the partially methylated alditol acetates were analyzed by GC–MS using a GCMS-QP2010 (Shimadzu) as earlier described (Braünlich et al., 2018), in which a Restek Rxi-5MS capillary column (30 m; 0.25 mm i.d.; 0.25 μm film) was attached. The estimation of relative amounts of each linkage type was related to the total mol percent of monosaccharides as determined by methanolysis as described above, and the effective carbon-response factors were considered for quantification of separated fragments based on integration of GC chromatograms (Sweet et al., 1975; Zou et al., 2017).

2.5. Molecular weight determination

The homogeneity and the weight-average molecular weight (*Mw*) of samples (2 mg/mL, 0.5 μL) were determined by SEC on Superose™ 6 (Amersham Biosciences, 10 × 300 mm) combined with the Äkta FPLC system. A calibration curve was prepared using dextran polymers with different *Mw* (5.6, 19, 50, 80, 150, 233, and 475 kDa, Pharmacia). Standards and samples were eluted with 10 mM NaCl, and 0.5 mL fractions were collected. The retention volume was converted to molecular weight based on the calibration curve provided by standards above.

2.6. NMR spectroscopy

^1H NMR (with continuous-wave presaturation, pulse program "zgpr"), ^{13}C NMR (pulse program "zrestse.dp.jcm800"), HMBC (pulse program "awhmbcgplpndqfpr" and "awshmbcctetgpl2nd.m"), HSQC (pulse program "awhsqcedetgpsisp2.3-135pr" and "awshsqc135pr") and COSY (pulse program "cosygpprqf") spectra of purified polysaccharides dissolved in 600 μL D_2O (99.9%, Sigma) were acquired on a Bruker Advance III HD 800 MHz spectrometer equipped with a 5-mm cryogenic CP-TCI z-gradient probe at 60 °C (Bruker, Rheinstetten, Germany). Spectra were analyzed by MestReNova software (Ver.6.0.2, Mestrelab Research S.L., Spain) and calibrated relative to sodium 2,2-dimethyl-2-silapentane-5-sulfonate at 0 ppm.

2.7. Complement fixation assay

The complement fixating activity of plant-derived polysaccharides has been used as an indicator for their potential effect on the immune system, which is measured based on inhibitory effects of hemolysis of antibody sensitized sheep red blood cells (SRBC) by human sera (Michaelsen et al., 2000) (Method A). A published highly active pectin from the aerial parts of *Biophytum petersianum* Klotzsch (Grønhaug et al., 2011), BPII, was used as the positive control. The 50% inhibition of hemolysis (ICH_{50}) of tested samples are obtained according to dose-response curves. A lower ICH_{50} value means a higher complement fixation activity. All samples were analyzed in duplicates in three separate experiments.

2.8. Anti-inflammatory effects on porcine jejunum epithelial cells (IPEC-J2)

2.8.1. Cell culture

IPEC-J2 cells were obtained from the Shanghai Institutes of Biological Sciences, Chinese Academy of Sciences (Shanghai, China), and were cultured in DMEM/F-12 medium (Beijing Solarbio Science & Technology Co., Ltd.), containing 10% fetal bovine serum (FBS, Thermo Fisher Scientific (China) Co., Ltd) and 1% penicillin-streptomycin (100 U/mL, Beijing Solarbio Science & Technology Co., Ltd.). They were maintained in a cell incubator with 5% CO_2 at 37 °C.

2.8.2. Cell viability and treatment

Cells were plated in 96-well cell plates (5×10^3 cells per well), and final concentrations of 20 μg/mL of AL-N, AL-I, AL-I-I and AL-I-II were added and co-cultivated for 24 h for the measurement of cell viability. The cytotoxic effects of all samples were assessed by Cell Counting Kit-8 reagent (CCK-8, Dojindo, CK04-11, Minato-ku, Tokyo, Japan) according to the manufacturer's instruction.

20 μg/mL LPS (Sigma-Aldrich, USA, purity ≥99%) was employed to induce inflammation on IPEC-J2 in a 6-well plate (5×10^3 cells per well) for 12 h. Then all samples were supplemented at final concentrations of 20 μg/mL in medium for the screening of the anti-inflammatory activity. High-yield acidic polysaccharides were further tested for a comprehensive comparison of anti-inflammatory activities among different fractions. Cells treated with LPS and medium were set as control cells, and those with only medium were negative control. After another 12 h of co-cultivation, all wells were rinsed with PBS, and total RNA was collected with Trizol Reagent (Biomed, RA101-12, China) for further analysis.

2.8.3. qRT-PCR

Total RNA of all collected cells was isolated using Trizol Reagent, and reverse transcribed into cDNA using M-MLV 4 First-Strand cDNA Synthesis Kit (Biomed, RA101-12, China). All real-time PCR analysis were

performed by SYBR Premix Ex Taq™ II (Tli RNaseH Plus) (Mei5Bio, China), and the gene expressions were quantified as relative regulation fold compared with *β-actin* (normalizing reference). Primers of all genes were shown in Table S1.

2.9. Statistical analysis

All experimental data were expressed as the mean ± S.D., and analyzed using one-way analysis of variance and Duncan test (IBM SPSS Statistics version 24, IBM Corp., Armonk, New York, USA).

3. Results and discussion

3.1. Isolation and purification of polysaccharide fractions from *A. carmichaelii* leaves

A crude polysaccharide, ALP, extracted from the dried leaves of *A. carmichaelii* was obtained, making up approximately 4.2% of the dried plant mass (2.1 g/50 g). This is in accordance with a previous study, reporting the presence of 4.9% polysaccharide in leaves of *A. carmichaelii* (Ou et al., 2013). As shown in Fig. 1 and by elution profiles in Fig. 2, one neutral fraction, AL-N (Fig. 2A), and one acidic fraction, AL-I (Fig. 2B), were obtained after anion exchange chromatography, with yields of 1.7% and 63.8% of ALP, respectively. The remaining amount of ALP might consist of undissolved compounds left in the filter before applying to IEC and colored compounds bound in the ANX Sepharose matrix. AL-I was further fractionated by SEC based on *Mw* difference, and two purified polysaccharides, named AL-I-I and AL-I-II, were obtained (Fig. 2C). Extraction yields are shown in Table 1. There was no detectable phenolic content in these fractions as assessed by the Folin-Ciocalteu test (Singleton & Rossi, 1965), and less than 1% of protein was detected (Table 1).

Table 1
Carbohydrate yields, weight-average *Mw*, and contents of protein in polysaccharide fractions isolated from *Aconitum carmichaelii* leaves.

	AL-N	AL-I-I	AL-I-II
Yields[a]	1.7%	19.7%	40.0%
Mw/kDa[b]	10.2	169.1	41.6
Total protein[c]	0.6%	1.0%	0.9%

[a] Yields related to the weight of the crude polysaccharide fraction ALP.
[b] Determined by SEC with a calibration curve of dextran standards (Section 2.5).
[c] Determined by Bio-Rad protein assay (Bradford, 1976).

3.2. Molecular weights of polysaccharide fractions

Homogeneity and weight-average molecular weight *Mw* of AL-N, AL-I-I and AL-I-II were determined by gel filtration (Fig. 2D), and is shown in Table 1. AL-N was considered a homogeneous fraction with lowest *Mw* among all fractions, as shown after applying on both Superose 6 (*Mw* range 5×10^3 to 5×10^6 Da, Fig. 2D) and Sephacryl S-100 High Resolution (*Mw* range 1×10^3 to 1×10^5 Da, Fig. 2E) columns. AL-I-I with a *Mw* of 169.1 kDa was the fraction with highest *Mw*. A huge *Mw* variation was also observed in acidic heteropolysaccharides isolated from the roots of *A. carmichaelii*, with *Mw* ranging from 5.8 kDa to more than 1000 kDa (Gao, Bia, et al., 2010).

3.3. Monosaccharide composition of polysaccharide fractions from *A. carmichaelii* leaves

The monosaccharide composition of AL-N, AL-I-I and AL-I-II were analyzed by GC as TMS derivatives of methylated monomers, and are presented in Table 2. The GC chromatograms are shown in Fig. S1. In AL-N, Glc (37.2 mol%) and Man (25.0 mol%) were the predominant monosaccharides, followed by Ara, Xyl, Gal and Fuc. A minor amount of GalA was detected in AL-N, and this could be due to methyl esterification of the uronic acid. The acidic heteropolysaccharides, AL-I-I and AL-

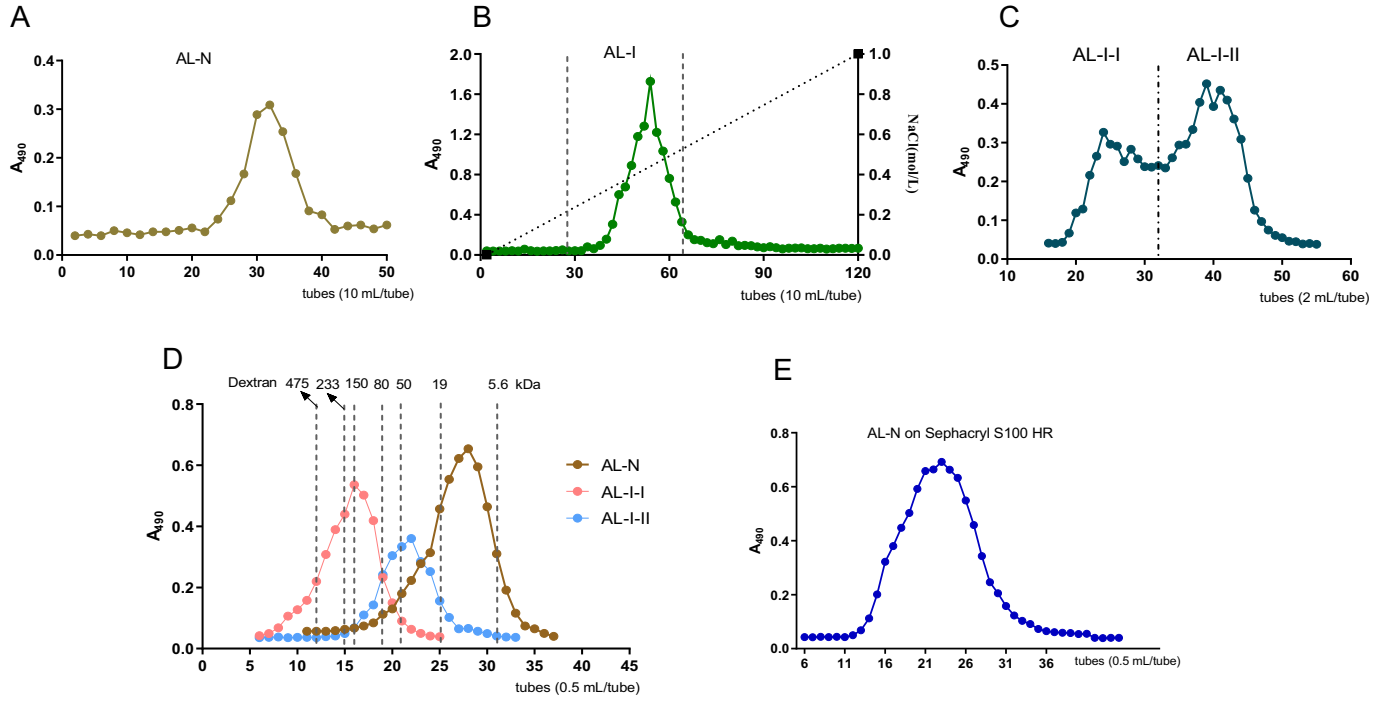

Fig. 2. The elution profiles of polysaccharides fractions AL-N, AL-I, AL-I-I and AL-I-II from *A. carmichaelii* leaves. Anion exchange chromatography elution profile of AL-N (A) and AL-I (B) on ANX Sepharose; Size exclusive chromatography elution profile of AL-I-I and AL-I-II on Superdex 200 (C), of AL-N, AL-I-I and AL-I-II on Superose 6 (D), and of AL-N on Sephacryl S100 HR (E).

Table 2
The monosaccharide composition (mol%) of polysaccharide fractions from *Aconitum carmichaelii* leaves.

	AL-N	AL-I-I	AL-I-II
Ara	12.7	28.0	5.9
Rha	0.4	7.2	5.2
Fuc	2.2	0.6	1.3
Xyl	12.7	5.2	5.4
Man	25.0	0.5	0.3
Gal	9.0	21.4	3.8
Glc	37.2	2.6	3.0
GlcA	n.d.	1.3	0.8
GalA	1.0	33.2	74.3

Note: mol% related to total content of the monosaccharides Ara, Rha, Fuc, Xyl, Man, Gal, Glc, GlcA, and GalA. n.d. = not determined.

I-II were composed of almost the same monosaccharides, but in different ratios. Both of them had a high proportion of GalA, but also neutral monosaccharides. Ara, Gal and Rha were the main monomers in addition to GalA in AL-I-I, while AL-I-II mostly consisted of GalA with lesser amounts of the neutral ones. These compositions are typical of pectic polysaccharides (Kaczmarska et al., 2022; Zaitseva et al., 2020).

As the first study on the structural characterization of polysaccharides from *A. carmichaelii* leaves, this study shows differences in the polysaccharide composition in leaves compared to those isolated from roots. Glucans and other neutral heteropolysaccharides mainly composed of Glc have been reported from roots of *A. carmichaelii* (Gao, Bia, et al., 2010; Wang et al., 2016; Yang et al., 2020; Zhao et al., 2006), but no polysaccharides consisting mainly of Man, Ara and/or Xyl have been reported so far. A possible pectin containing mainly Glc, Ara, Gal, and 5.7–33.5% of GalA have been reported in the roots by Gao, Bia, et al. (2010). However, no detailed structural analysis that can give evidence for the presence of pectin in any plant parts of *A. carmichaelii* have been performed.

3.4. Structural characterization of polysaccharides from leaves of *A. carmichaelii*

3.4.1. Glycosidic linkages

Based on monosaccharide compositions, the glycosidic linkage types of AL-N, AL-I-I, and AL-I-II were determined by GC–MS after permethylation, and are shown in Table 3. The GC chromatograms of fragments and MS spectra of each corresponding fragment are shown in Fig. S2.

The major linkage patterns of AL-N were 1,4-linked Man*p* (22.4 mol %) and 1,4-linked Glc*p* (22.8 mol%), both monomers also having 1,4,6-linkages. Ara*f* was present mainly as terminal and 1,5-linked units, in addition to 1,3,5-linked residues. Xyl*p* and Gal*p* were present as terminal units and as linear chains, 1,2-linked and 1,3-linked respectively. As reported previously, hemicellulose or storage polysaccharides in primary plant cell wall (Fry, 2011; Hayashi & Kaida, 2011; Nishinari et al., 2007) includes mannans (a backbone rich in or entirely composed of 1,4-linked β-Man*p* and occasionally carrying terminal β-Gal*p* at *O*-6 as side chains), glucomannans (mannans with 1,4-linked β-Glc*p* within the backbone and/or terminal β-Gal*p* at *O*-6 of Man*p*) and xyloglucans (composed of 1,4-linked β-Glc*p* as backbone and branched at *O*-6 with terminal α-Xyl*p*, and/or 1,2-linked Xyl*p* connected with terminal Gal*p*). According the xyloglucan models described by Fry et al. (1993), the specific structure of the xyloglucan in AL-N could be XXLG (X, α-$_D$-Xyl*p*-(1 → 6)-β-$_D$-Glc*p*; L, β-$_D$-Gal*p*-(1 → 2)-α-$_D$-Xyl*p*-(1 → 6)-β-$_D$-Glc*p*; G, β-$_D$-Glc*p*) or XLXG model due to the ratio of relative amounts of T-α-Xyl and1,2-linked α-Xyl (7.7:4.7, Table 3). Given the homogenous composition observed in Fig. 2D and Fig. 2E, AL-N might be a mixture of mannans, xyloglucans and/or glucomannans and minor amounts of arabinogalactan with similar *Mw*, as depicted in Fig. 4. The rather low yield of this fraction compared to the high yield of AL-I (Table 1) was the reason for not perform in further studies on AL-N.

Table 3
Glycosidic linkage types (mol%) present in polysaccharide fractions from leaves of *Aconitum carmichaelii*.

Linkage types	Rt/min	Primary fragments	AL-N	AL-I-I	AL-I-II
Ara*f*					
T-	12.41	45, 118, 161, 162	4.1	21.6	4.8
1,3-	14.76	45, 118, 233	trace	1.1	trace
1,5-	15.53	118, 162, 189	4.8	3.3	trace
1,3,5-	17.55	118, 261	2.6	1.8	trace
Rha*p*					
T-	13.31	118, 131, 162, 175	n.d	trace	3.7
1,2-	15.53	131, 190	n.d	3.9	trace
1,2,4-	17.91	190, 203	n.d	2.8	trace
Fuc*p*					
T-	14.04	118, 131, 162, 175	2.2	trace	1.3
Xyl*p*					
T-	13.31	117, 118, 162	7.7	5.2	4.2
1,2-	15.71	117, 130, 190	4.7	n.d	n.d
1,4-	15.71	118, 162, 189	n.d	n.d	1.2
Man*p*					
1,4-	19.05	45, 118, 162, 233	22.4	n.d	n.d
1,4,6-	21.60	118, 162, 261	1.5	n.d	n.d
Gal*p*					
T-	17.17	45, 118, 162, 205	3.2	1.6	1.2
1,3-	19.42	118, 161, 234, 277	2.4	2.3	trace
1,4-	19.03	45, 118, 162, 233	n.d	1.0	trace
1,6-	20.41	118, 162, 189, 233	trace	1.7	trace
1,3,6-	22.63	118, 189, 234, 305	trace	7.1	trace
1,3,4-	20.71	45, 118, 305	n.d	1.0	n.d
1,4,6-	22.00	118, 162, 261	trace	1.4	trace
1,3,4,6-	23.4	118, 333	1.1	5.2	trace
Glc*p*					
T-	16.62	45, 118, 161, 162, 205	1.1	n.d	1.4
1,3-	18.93	45, 118, 161, 234, 277	2.3	trace	n.d
1,4-	19.22	45, 118, 162, 233	22.8	1.9	1.5
1,4,6-	21.80	118, 162, 261	10.4	trace	trace
Glc*p*A					
T-	16.62	47, 118, 161, 162, 207	n.d	1.1	trace
Gal*p*A					
T-	17.17	47, 118, 162, 207	trace	trace	2.3
1,4-	19.03	47, 118, 162, 235	trace	27.9	62.6
1,2,4-	21.19	47, 190, 235	n.d	trace	1.7
1,3,4-	20.71	47, 118, 307	n.d	4.6	8.0

Note: trace, relative amount less than 1.0%, n.d, not detected.

The acidic polysaccharides AL-I-I and AL-I-II consists of monomers and glycosidic linkages typically found in pectic polysaccharides. The main linkage types for both AL-I-I and AL-I-II was 1,4-linked Gal*p*A, most probably coming from a homogalacturonan (HG) domain that is often present in intercellular tissues as part of plant cell wall (Voragen et al., 2009). The HG region can be substituted by terminal Xyl*p*, as xylogalacturonan (XGA) (Patova et al., 2021; Wang et al., 2019), as well as by terminal Fuc*p* at position C-3 of 4)-Gal*p*A-(1 → (Braünlich et al., 2018), which also can be the case in both AL-I-I and AL-I-II. The HG region is longer in AL-I-II than AL-I-I, as it contains 35 mol% more of 1,4-linked Gal*p*A (Table 3).

Further, several types of neutral monosaccharides were found in AL-I-I, such as 1,2- and 1,2,4-linked Rha*p*, terminal- (T-), 1,5- and 1,3,5-linked Ara*f*, and 1,3- and 1,3,6-Gal*p*. These linkage patterns indicate a possible presence of type I rhamnogalacturonan (RG-I), arabinan and arabinogalactan (AG) domains, respectively (Kaczmarska et al., 2022; Voragen et al., 2009). 1,3,4,6-linked Gal*p* (5.2 mol%) detected in AL-I-I could be terminated with Ara*f*, as has been described in other pectic polysaccharides (Braünlich et al., 2018; Shen et al., 2021; Zhang, Li, et al., 2020). More than 20 mol% of terminal Ara*f* was found in AL-I-I, which might be due to arabinan and AG domains, as the total amount (20.3 mol%) of branched monomers including 1,3,5-Ara*f*, 1,3,4-Gal*p*, 1,3,6-Gal*p* and 1,3,4,6-Gal*p* (connected with two Ara*f*) was close to the amount of terminal Ara*f*. Both AG type II (AG-II) moieties, 1,3 linked Gal*p* units branched at C-6 (7.1 mol%), and AG type I (AG-I) moieties, 1,4-linked Gal*p* blocks branched at C-3 (1.0 mol%), were present in AL-I-

I (Table 3). The ratio of AG-II: AG-I: arabinan could be approximate 7:1:1 according to the relative amounts of these branching units. These results illustrated a highly branched structure of AL-I-I. For AL-I-II, a longer HG backbone was found, and therefore more moieties would be attached to C-3 of Gal*p*A compared to AL-I-I. Few neutral side chains were shown for AL-I-II, as only trace amounts of 2,4)-Rha*p*-(1 → units were detected, and consequently, less amount of arabinan or AG domains were revealed. Terminal Glc*p*A could be located on the end of arabinogalactan side chains (Makarova et al., 2016; Zhang, Li, et al., 2020).

3.4.2. NMR analysis

The structure of AL-I-I and AL-I-II were further analyzed by NMR. The data were interpreted by comparing and matching chemical shift

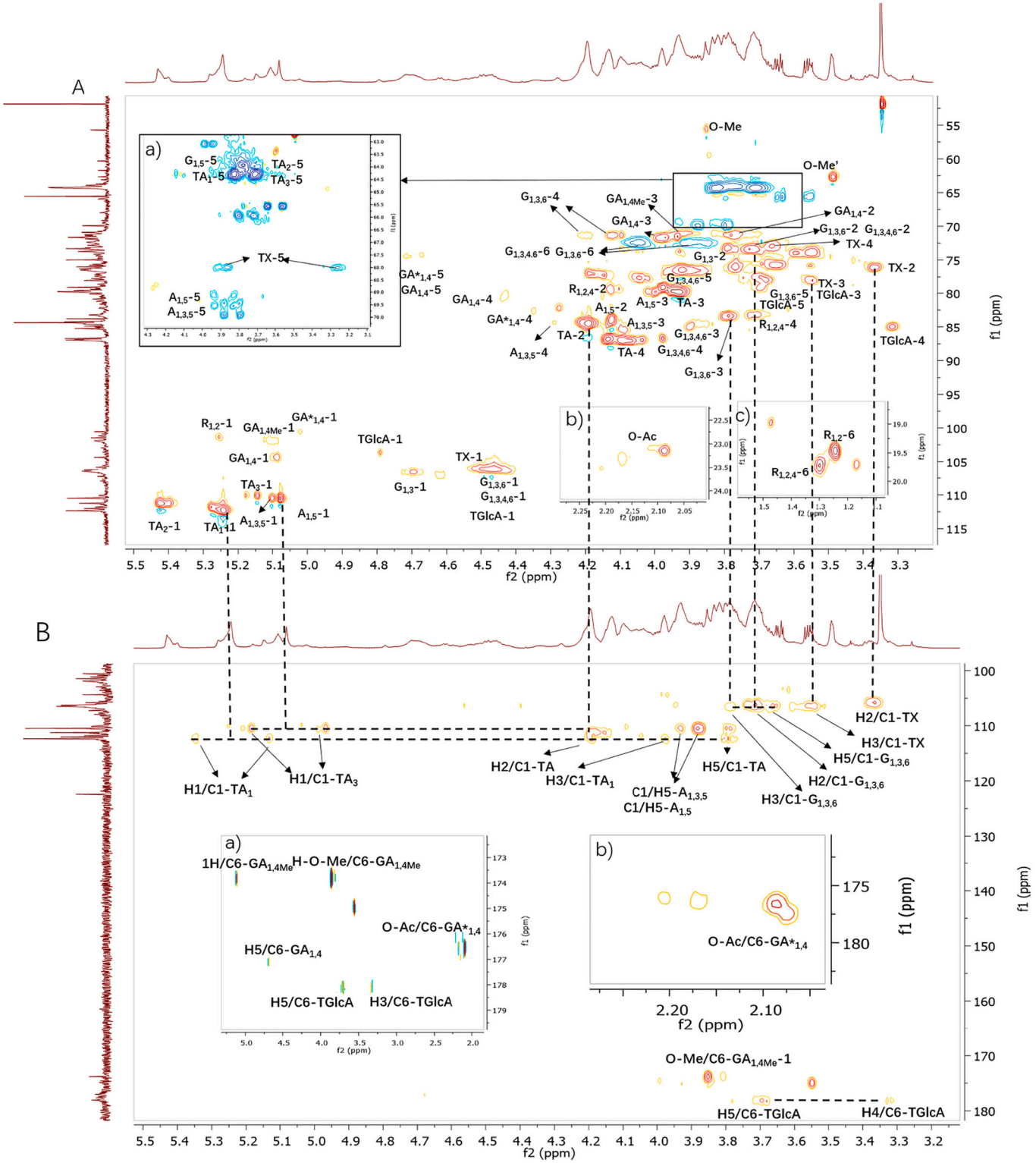

Fig. 3. 2D NMR spectra of pectic polysaccharides from leaves of *A. carmichaelii*. HSQC (A) and HMBC spectra (B) of AL-I-I, and HSQC (C) and HMBC spectra (D) of AL-I-II. Inserted plots were selective HSQC or HMBC spectra zooming in specific chemical shift range.

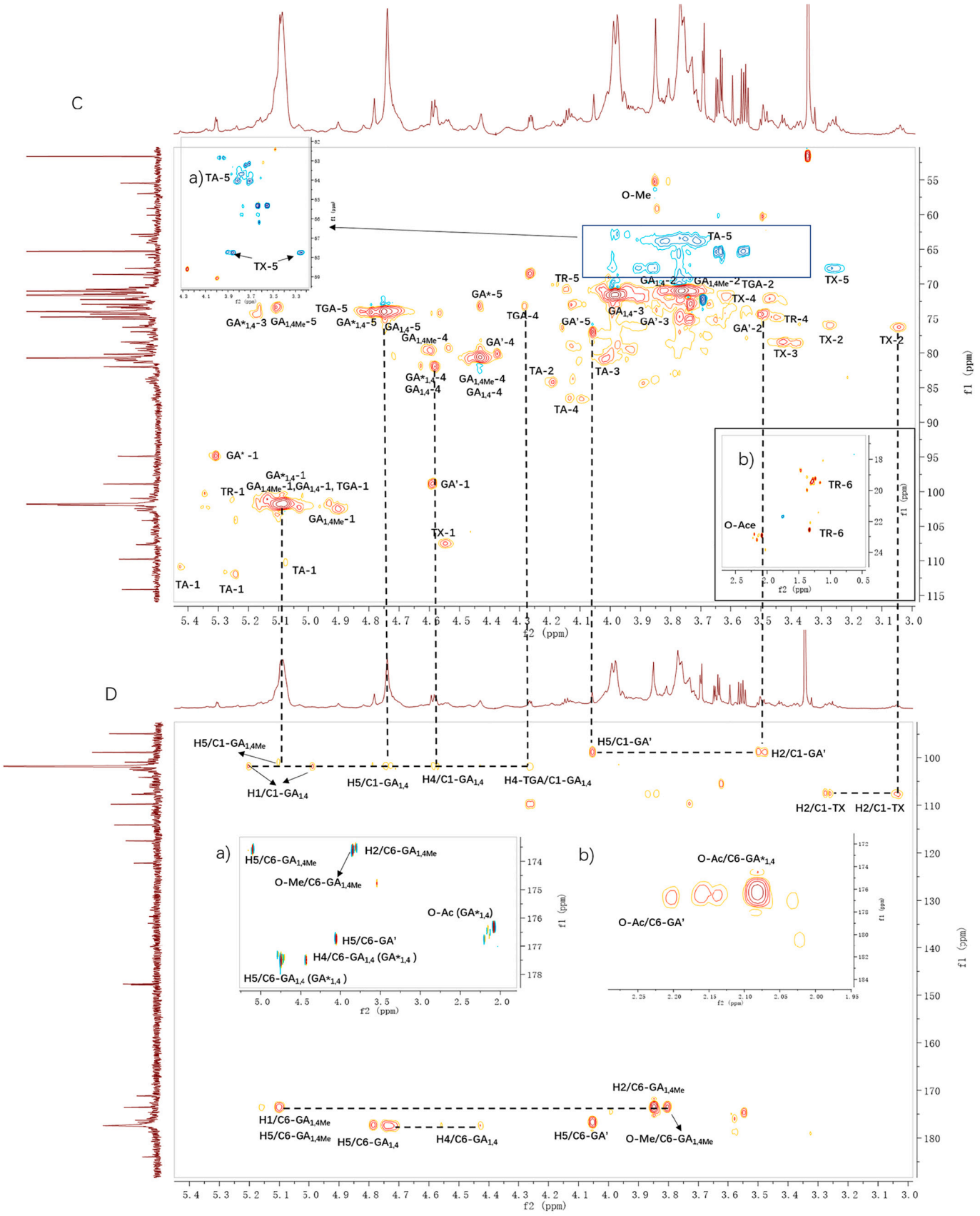

Fig. 3. (*continued*).

values from the 1D spectra ^{1}H and ^{13}C (Fig. S3A and B, Fig. S4A and B,), and the 2D spectra COSY (Fig. S3C and Fig. S4C), HSQC and HMBC (Fig. 3). Space correlation of AL-I-I including ROESY and NOESY are presented in Fig. S3D and Fig. S3E respectively, but only a few correlations of AL-I-II were detected. Typical residues were assigned based on the methylation analysis and previously reported literature (Huang, Li, et al., 2021; Huang, Peng, et al., 2021; Makarova et al., 2016; Patova et al., 2021; Patova et al., 2019; Shakhmatov et al., 2019; Shakhmatov et al., 2015; Zhang, Li, et al., 2020; Zou et al., 2021; Zou et al., 2020), and the values of the chemical shifts are presented in Table 4. However, signals from trace residues and bound correlations between monomers are hard to be recorded.

The anomeric region between δ 5.1 to δ 5.8 in ^{1}H NMR and δ 98 to δ 103 in ^{13}C NMR are signals of sugar residues with α-configuration, while those in β-configuration commonly appear in δ 4.4 to 4.8 and δ 103 to 106 (Yao et al., 2021). Peaks in the region δ 1.1 to 1.4 in ^{1}H NMR and δ 16 to 18 ^{13}C NMR indicated the presence of —CH_3 of Rha, while those at δ 2.0 to 2.2 and δ 18 to 22, and δ 3.3 to 3.8 and δ 55 to 61 suggested the presence of acetyl (CH_3CO—) and methyl units (—OCH_3) respectively (Yao et al., 2021). The rest of the high-intense peaks could be assigned to protons and carbons from C-2 to C-5 or C-6 of monomers, and their chemical shifts change if they are in different chemical environment.

Many signals and cross peaks from Ara*f* can be detected due to its high concentration in **AL-I-I** based on results of methylation, therefore signals of anomeric carbon (C-1) at 103 to 112 ppm derived from furanose should be assigned to α-Ara*f* (Yao et al., 2021). As shown in Table 4 and Fig. 3A, the intense signals of H/C-atoms at δ 5.24/112.3 (**TA_1-1**), δ 5.42/111.2 (**TA_2-1**), and δ 5.14/110.1 (**TA_3-1**), belong to α-Ara*f*-(1 → residues (Makarova et al., 2016; Shakhmatov et al., 2015). They might differ in terms of their appendences to Gal*p*, or various substituted α-Ara*f* (Zhang, Li, et al., 2020). However, it was hard to distinguish these in this case, as correlations between H-1 of terminal Ara*f* and H-3/4/6 of substituted Gal*p* or H-3/5 of substituted Ara*f* were highly overlapped. In the current HSQC pulse program, a multiplicity edited with Distortionless Enhancement by Polarization Transfer (DEPT)-135 carbon experiment was set, in which the intensity of all protonated carbons depends on the magnitude of the flip angle and the number of protons attached to a carbon. As a result, after polarization transform, carbon signals from methine (CH) and methyl (CH_3) groups are generally positive, but those from methylene (CH_2) groups are negative. For Ara*f*, signals of C-5 and H-5 (CH_2-OH) were detected as negative (blue) cross points at 64 to 70 ppm (Fig. 3A). The cross peaks related to C-1 of Ara*f* in HMBC helped to assign the protons located at other carbons in the same sugar ring, such as H-2 and H-3. For example, protons at 4.19, 3.98 and 3.82 ppm correlated to C-1 at 112.3 ppm in HMBC were assigned to H-2, H-3 and H-5 of TA_1 respectively (Fig. 3B), and correlations among them were also observed as cross peaks in COSY and space correlations in ROESY (Fig. S3D) and NOESY (Fig. S3E). However, protons correlated to C-1 at 110.5 ppm in HMBC (residues at δ 110.5/3.88, δ 110.5/3.80 and δ 110.5/3.93, Fig. 3B) should be assigned to H-5 of *O*-5-substituted Ara*f*, due to the downfield chemical shifts of their attached carbons at 69.9 (δ 3.80, 3.88/69.9, **$A_{1,5}$-5**) and 69.5 ppm (δ 3.83, 3.93/69.5, **$A_{1,3,5}$-5**) in HSQC compared to the carbons of terminal Ara*f* at 63–64 ppm (Fig. 3A) (Shakhmatov et al., 2015; Zhang, Li, et al., 2020; Zou et al., 2021), which were also proved by the H/C correlations at δ 5.08/69.9 in HMBC (Fig. S3F, a).

Highly branched arabinogalactans were further confirmed by the residues of →3,4,6)-β-Gal*p*-(1 → (**$G_{1,3,4,6}$-1**), →3,6)-β-Gal*p*-(1 → (**$G_{1,3,6}$**) and →3)-β-Gal*p*-(1 → (**$G_{1,3}$-1**) according to high intense H/C correlations of typical β-pyranose at δ 4.49/106.3 (**$G_{1,3,4,6}$-1**), δ 4.46/105.9 (**$G_{1,3,4,6}$-1**), and a weak one at δ 4.69/106.5 (**$G_{1,3}$-1**) in HSQC spectrum (Fig. 3A), and those between H-2/3/5 and C-1 in HMBC (Fig. 3B), as well as proton-proton correlations between H-1 and H-2 in COSY (Fig. 3SC), and between H-1 and H-2/3/6 in ROESY (Fig. 3SD) and NOESY (Fig. S3E), which were in line with earlier reported values (Shakhmatov et al., 2018; Shakhmatov et al., 2015; Zhang, Li, et al., 2020). A downfield chemical shift of H/C-atoms of *O*-4 substituted Gal*p* was also observed at δ 3.98/86.7 in HSQC (Fig. 3A, **$G_{1,3,4,6}$-4**) (Zhang, Li, et al., 2020).

Furthermore, the anomeric spin systems H-1/C-1 at δ 5.26/101.4 was assigned to 1,2-α-Rha*p* (**$R_{1,2}$**), and the signal of H-2 were assigned due to the proton-proton correlations in COSY (Fig. 3C) and NOESY (Fig. S3E). Signals of C-4 and C-5 of Rha*p* were appointed according to H-6/C-4 correlations at δ 1.24/75.0 and δ 1.30/83.2 and H-6/C-5 correlations at δ 1.24/71.8 and δ 1.30/71.2 in HMBC (Fig. S3F, b), based on values reported in previous studies (Shakhmatov et al., 2018; Shakhmatov et al., 2019). Due to the relative low amounts of Rha*p* residues in AL-I-I, some proton signals were not able to detected. Regarding the signals of H/C-atoms at δ 5.09/104.3, and weak ones at δ 5.11/101.8 and δ 5.02/100.6 in HSQC, they belong to anomeric H/C atoms of 1,4-α-Gal*p*A (**$GA_{1,4}$**), 1,4-α-Gal*p*A-6-*O*-Me (**$GA_{1,4Me}$**) and 4-α-3-*O*-Ac-Gal*p*A (**$GA^{*}_{1,4}$**) respectively (Patova et al., 2019; Shakhmatov et al., 2019; Zou et al., 2020). Peaks in the downfield region in ^{13}C NMR at 173.8, 177.1 and 177.6 ppm should be assigned to C-6 of Gal*p*A. Other protons related to C-6 of Gal*p*A in HMBC were assigned to H-3/4/5 (Fig. 3B). The ROESY spectrum also shows cross peaks among H-1, H-2 of 1,2-linked Rha*p* and H-1 and H-3 of 1,4-linked Gal*p*A, indicating the presence of RG-I backbone moiety →4-α-Gal*p*A-(1,2)-α-Rha*p*-(1 → (Fig. S3E) (Shakhmatov et al., 2016). Besides the cross peak of residue ***O*-Ac** in HSQC, the presence of acetyl esterified Gal*p*A was evidenced by the carbon signal of carboxyl in acetyl units due to the cross peak at δ 2.09/176.3 in HMBC (Fig. 3B) (Patova et al., 2019). According to linkage analysis 1,3,4-linked Gal*p*A was found in AL-I-I (Table 3), which could indicate a substitution of an acetyl-group at *O*-3 of Gal*p*A (4-α-3-*O*-Ac-Gal*p*A). However, due to the relative low amount of 1,3,4-linked Gal*p*A, which would give the same PMAA fragments during permethylation as 4-α-3-*O*-Ac-Gal*p*A, the downfield shifts of proton H-3/C-3 was not detected (Kostálová et al., 2013). The existence of methyl esterified Gal*p*A (1,4-α-Gal*p*A-6-*O*-Me) was illustrated by cross peaks at δ 3.85/55.6 in the HSQC spectra (**O-Me**, Fig. 3A). However, the spin system reported for Gal*p*A methyl ester residues with downfield shifts of H-5 from about 4.7 to about 5.10 was not detected. But the shift of C-6 was observed at 173.8 ppm compared to those of non-esterified Gal*p*A at around 177 ppm, as well as correlation between *O*-Me and carboxyl group in HMBC at δ 3.85/173.8 (**H-O-Me/C6-$GA_{1,4Me}$**) (Fig. 3B) (Rosenbohm et al., 2003; Shakhmatov et al., 2016; Zou et al., 2020).

The position of the anomeric proton and carbon for terminal Xyl*p* (**TX-1**) was identified due to the signals at δ 3.37/105.8 (**H2/C1-TX**), δ 3.55/106.1 (**H3/C1-TX**) in HSQC (Fig. 3A) as earlier described (Patova et al., 2021), and strong correlations at δ 4.49/3.37 and δ 4.53/3.04 in COSY (Fig. S3C). The terminal Xyl could be attached to the HG region at position 3 of Gal*p*A (Patova et al., 2021; Wang et al., 2019) or to galactan domains at position 6 of Gal*p* (Zhang et al., 2019). Similarly, the assignment of methyl esterified Glc*p*A was deduced by spin systems at δ 3.49/62.7 (**O-Me′**) and δ 3.32/84.9 (**TGlcA-4**) in HSQC (Fig. 3A), residues at δ 3.32/178.01 (**H4/C6-TGlcA**), δ 3.69/178.1 (**H5/C6-TGlcA**), δ 3.49/84.9 (*O*-Me/C4-TGlcA, Fig. S3F, c) and δ 3.32/78.0 (H4/C3-TGlcA, Fig. S3F, c) in HMBC spectra (Fig. 3B), and proton-proton correlations in COSY (**H1/H2-TGlcA**), which were in agreement with values of chemical shifts published by Makarova et al. (2016) and Zhang, Li, et al. (2020), as terminal units of galactans or arabinogalactans.

The assignment of **AL-I-II** is easier than for AL-I-I as it consisted of more than 60 mol% of Gal*p*A. Briefly, C-1 and C-6 of α-Gal*p*A gave intense signals in anomeric regions in HSQC (such as residues **$GA_{1,4Me}$-1, $GA_{1,4}$-1** and **TGA-1** in Fig. 3C), and cross peaks in the anomeric (such as residues **H5/C1-$GA_{1,4}$** and **H4/C1-$GA_{1,4}$** in Fig. 3D) and downfield areas (such as residues **H1/C6-$GA_{1,4Me}$, H5/C6-$GA_{1,4Me}$** and **H5/C6-$GA_{1,4}$** in Fig. 3D) in HMBC. Most proton signals correlated with H-1 of Gal*p*A were appointed to H-2 by cross peaks in COSY (Fig. S2C), and their correlations to C-1 of Gal*p*A in HMBC (Fig. 3D). Carbon signals correlated to H-1 were assigned to C-2/3/4 of Gal*p*A (Fig. S4D, a). Some of the 1,4-α-Gal*p*A residues were *O*-6 methyl esterified. Because of the downfield shifts of H-5 from about 4.7 ppm to about 5.10 ppm and the

Table 4
^{1}H and ^{13}C NMR chemical shifts (ppm[a]) assignment of AL-I-I and AL-I-II.

Residues (Abb.)		H1/C1	H2/C2	H3/C3	H4/C4	H5/C5	H6/C6	O-Me/O-Me′/O-$\underline{C}H_3$	O-Ac/$\underline{C}H_3CO$ ($CH_3\underline{C}O$)	Ref.
AL-I-I										
α-Ara*f*-(1→	(**TA$_1$**)	5.24/ 112.3	4.19/ 84.5	3.98/ 79.1	4.14/86.8	3.71, 3.82/64.3				
α-Ara*f*-(1→	(**TA$_2$**)	5.42/ 111.2	4.19/ 84.5	3.98/ 79.1	4.14/86.8	3.82/63.7				
α-Ara*f*-(1 →	(**TA$_3$**)	5.14/ 110.1 5.18/ 110.1	4.14/ 84.6	3.93/ 79.8	4.04/87.0 4.10/87.0	3.78/63.9 3.71, 3.82/64.3				(Makarova et al., 2016) (Shakhmatov et al., 2015) (Zou et al., 2021)
→5)-α-Ara*f*-(1→	(**A$_{1,5}$**)	5.08/ 110.5	4.12/ 83.9	4.00/ 79.8	4.20/85.2	3.80, 3.88/69.9				
→3,5)-α-Ara*f*-(1→	(**A$_{1,3,5}$**)	5.10/ 110.5	4.14/n. d.	4.10/ 85.4	4.29/84.4	3.80, 3.88/69.4 3.83, 3.93/69.5				
→2)-α-Rha*p*-(1→	(**R$_{1,2}$**)	5.26/ 101.4	4.10/ 79.4	3.93/ 73.7	3.43/75.0	n.d./71.8	1.24/19.5			(Shakhmatov et al., 2018; Shakhmatov et al., 2019)
→2,4)-α-Rha*p*-(1→	(**R$_{1,2,4}$**)	n.d.	4.10/ 79.4	4.10/ 73.3	3.71/83.2	n.d./71.2	1.30/19.7			
β-Xyl*p*-(1→	(**TX**)	4.49/ 105.8 4.53/ 106.1	3.37/ 76.1 3.04/n. d.	3.55/ 78.0	3.66/72.9	3.26, 3.87/68.0				(Patova et al., 2021)
→3)-β-Gal*p*-(1→	(**G$_{1,3}$**)	4.69/ 106.5	3.79/ 73.2	3.87/ 84.6	4.21/71.3	n.d.	3.82/63.7			(Shakhmatov et al., 2015; Shakhmatov et al., 2018)
→3,6)-β-Gal*p*-(1→	(**G$_{1,3,6}$**)	4.49/ 106.3	3.73/ 73.4	3.79/ 83.4	4.12/ 71.34.10/ 71.4	3.92/76.5	3.92, 4.04/72.4			
→3,4,6)-β-Gal*p*-(1→	(**G$_{1,3,4,6}$**)	4.46/ 105.9	3.73/ 73.4	3.90/ 85.0	3.98/86.7	3.69/77.5 3.65/75.7	3.92, 4.04/72.4			(Zhang, Li, et al., 2020).
→4)-α-Gal*p*A-6-*O*-Me-(1→	(**GA$_{1,4Me}$**)	5.11/ 101.8	3.83/ 71.0	3.93/ 71.5	4.43/80.2	n.d.	173.8	3.85/55.6		(Patova et al., 2019; Shakhmatov et al., 2018)
→4)-α-Gal*p*A-(1→	(**GA$_{1,4}$**)	5.09/ 104.3	3.78/ 71.3	3.97/ 71.7	4.44/80.7	4.67/74.2	177.0 177.1			
→4)-α-3-*O*-Ac-Gal*p*A-(1→	(**GA*$_{1,4}$**)	5.02/ 100.6	n.d.	n.d.	4.44/80.7	4.72/74.4	177.6		2.09/23.2 2.17/23.3 (176.3)	(Patova et al., 2019)
β-Glc*p*A-4-*O*-Me-(1→	(**TGlcA**)	4.46/n. d.	3.37/n. d.	3.55/ 78.0	3.32/84.9	3.69/78.9	178.1	3.49/62.7		(Makarova et al., 2016)
AL-I-II										
α-Ara*f*-(1→	(**TA**)	5.08/ 110.2 5.24/ 111.9 5.43/ 110.9	4.19/ 84.2 4.12/ 83.7	4.01/ 80.8 4.02/ 81.0	4.13/86.5 4.10/86.6	3.71, 3.81/64.0				(Makarova et al., 2016)
α-Rha*p*-(1→	(**TR**)	4.93/ 101.6	3.91/ 71.9	3.70/ 71.1	3.44/74.8	3.90/71.9 n.d./71.6	1.29/19.4 1.24/19.2			(Makarova et al., 2016)
β-Xyl*p*-(1→	(**TX**)	4.55/ 107.5 n.d./ 107.7	3.27/ 76.1 3.04/ 76.3	3.38/ 78.6 3.43/ 78.4	3.61/71.8 3.73/72.9	3.26, 3.86/67.8 3.90/67.7				(Patova et al., 2021)
α-Gal*p*A-(1→	(**TGA**)	5.03/ 102.3	3.77/ 71.0	3.98/ 71.5	4.28/73.2	4.75/74.0	177.4			(Shakhmatov et al., 2018) (Patova et al., 2021)
→4)-α-Gal*p*A-6-*O*-Me-(1→	(**GA$_{1,4Me}$**)	4.90/ 102.4 5.10/ 101.8 5.16/ 102.1	3.77/ 71.0 3.77/ 70.9 4.00/n. d. 3.83/ 71.0	3.80/ 72.7 3.98/ 71.5 3.61/ 71.8 3.91/ 72.0	4.43/80.6 4.60/79.6	5.11/73.4 5.16/74.1	173.5	3.85/55.3 3.85/59.1		(Shakhmatov et al., 2016)
→4)-α-3-*O*-Ac-Gal*p*A-(1→	(**GA*$_{1,4}$**)	5.08/ 101.7	4.06/n. d.	5.17/ 74.4	4.58/81.9 4.43/80.6	4.79/74.0	177.4		2.08/22.9 2.16/23.2 2.14/22.9 (176.3)	(Patova et al., 2021)
	(**GA$_{1,4}$**)				4.43/80.6		177.4			(Patova et al., 2021)

(*continued on next page*)

Table 4 (*continued*)

Residues (Abb.)		H1/C1	H2/C2	H3/C3	H4/C4	H5/C5	H6/C6	O-Me/O-Me′/O-$\underline{C}H_3$	O-Ac/$\underline{C}H_3CO$ ($CH_3\underline{C}O$)	Ref.
→4)-α-Gal*p*A-(1→		5.08/101.7	3.77/71.0	3.91/72.0		4.79/74.0 4.75/74.0				
→4)-α-Gal*p*A	(**GA***)	5.31/94.8	3.83/71.0	3.98/71.5	4.46/80.9	4.43/73.2	n.d.			
	→4)-β-Gal*p*A	(**GA′**) 4.59/98.8	3.49/74.3 3.45/74.8	3.77/74.1 3.73/75.0	4.38/80.1	4.06/77.0 3.92/76.2	176.6			

[a] Values of the chemical shifts were determined from the HSQC spectra of each sample (solvent: D_2O). n.d., not detected.

shifted signal of C-6 at 173.8 ppm for Gal*p*A methyl ester residues (Rosenbohm et al., 2003; Shakhmatov et al., 2016), the →4)-α-Gal*p*A-6-*O*-Me-(1 → residue was further identified by cross peaks at δ 3.85/55.3, δ 3.85/59.1 (**O-Me**) and δ 5.11/73.4, 5.17/74.4 (**$GA_{1,4Me}$-5**) in HSQC, and δ 3.85/173.5 (**O-Me/C6-$GA_{1,4Me}$**), δ 3.77/173.5 (**H2/C6-$GA_{1,4Me}$**) and δ 5.10/173.5 (**H1/C6-$GA_{1,4Me}$**) in HMBC. Some of 1,4-α-Gal*p*A of AL-I-II were acetyl esterified at *O*-3 of Gal*p*A according to cross peaks at δ 2.08/22.9, δ 2.14/23.2 and δ 2.14/22.9 in HSQC (**O-Ac**, Fig. 3C), δ 2.08/176.3 in HMBC (**O-Ac/C6-$GA^*_{1,4}$**, Fig. 3D), as well as downfield shifts of H/C-3 at δ 5.17/74.4 (Table 3). This is equivalent to results of previous studies (Kostálová et al., 2013; Patova et al., 2019). Particularly, a 4 → β-Gal*p*A was found in AL-I-II, since cross peaks of H/C at δ 4.59/98.8 (**GA′-1**), δ 4.38/80.1 (**GA′-4**) and δ 3.49/74.4 ppm (**GA′-2**) in HSQC, δ 4.06/98.8 (**H5/C1-GA′**), δ 3.49/98.8 (**H2/C1-GA′**), δ 4.06/176.7 (**H5/C6-GA′**) in HMBC (Fig. 3D) and H1/H2 and H2/H3 correlations in COSY (Fig. S4C) were detected, which also has been shown in other studies (Patova et al., 2019; Patova et al., 2021; Zou et al., 2020). The β-linkage was detected in AL-I-II due to the high-resolution 800 MHz NMR instrument, and it might be the reason that this structure has not been highly mentioned in most papers related to pectins. The signals of terminal β-Xyl*p* were also found in AL-I-II by similar cross peaks as described above in AL-I-I. However, few signals of *O*-5-substituted Ara*f* and *O*-6-substituted Gal*p* were found due to the low amounts of these linkage types in AL-I-II (Table 4), which was why less —CH_2— signals at around 68–72 ppm were observed in the inserted plot in HSQC (Fig. 3C). In addition, the residues **TR-1**, **TR-2**, and **TR-4** in HSQC demonstrated the presence of terminal α-Rha*p*, as well as H/C cross peaks at δ 1.29/71.9, δ 1.29/74.8 and δ 1.24/71.6 in HMBC (Fig. S4D, b) and H/H cross peak at δ 1.29/3.90 in COSY spectra (not shown), as described in earlier published studies (Cui et al., 2007; Makarova et al., 2016). Likewise, the terminal α-Rha*p* residue might be located at the end of Glc*p*A, Gal*p*, or Ara*f* containing side chains, since around 3 mol% in total of all trace linkages belonging to Ara*f* and Gal*p* were measured in methylation analysis, such as 1,2-, 1,3-, 1,3,5-linked Ara*f* and 1,6-, 1,3,6- and 1,4,6-linked Gal*p*.

Thus, according to the aforementioned results and NMR elucidation, both AL-I-I and AL-I-II could be typical pectin polysaccharides with both methyl- and acetyl-esterified α-GalA units, as depicted in Fig. 4. According to the known structure of plant-derived pectic polysaccharides (Kaczmarska et al., 2022; Zaitseva et al., 2020) and the results of glycosidic linkages and NMR analysis above, AL-I-I was probably mainly composed of AG-II and arabinan as side chains of a RG-I core chain besides a HG backbone. The correlations in NMR were however too weak to indicate how the side chains were connected to the RG-I core and HG backbone. AL-I-II consisted of a longer HG backbone with substituents at α-3-*O*-Gal*p*A.

So far, no structural characterization of pectins in any plant part of *A. carmichaelii* has been reported, besides the description of a possible

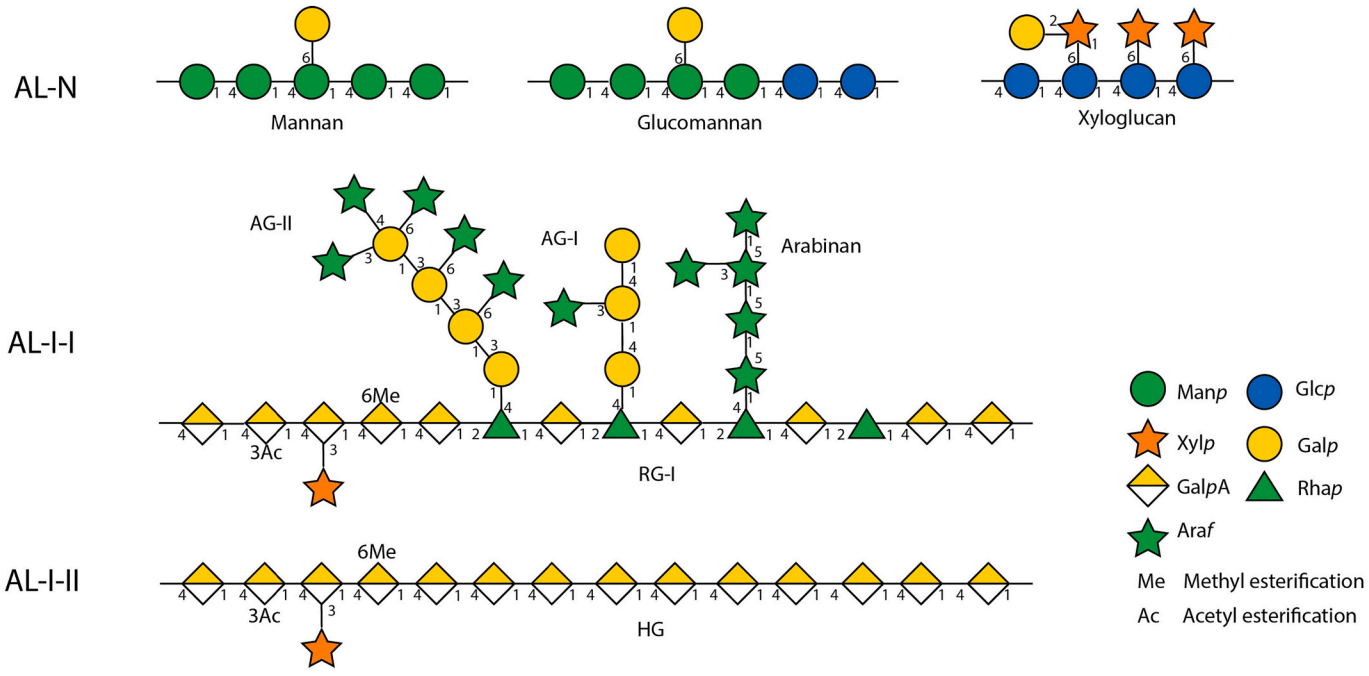

Fig. 4. Proposed structures of polysaccharides from *A. carmichaelii* leaves. HG, homogalacturonan; RG-I, type I rhamnogalacturonan; AG-II, type II arabinogalactan; AG-I, type I arabinogalactan. Graphical symbols are depicted according to the symbol nomenclature for glycans (SNFG) (Varki et al., 2015).

pectin by Gao, Bia, et al. (2010) due to a detectable amount of GalA in polysaccharides from the roots. In other *Aconitum* plants, various types of polysaccharides have been identified in the roots of *A. coreanum*, including a type II rhamnogalacturonan (RG-II) polysaccharide (Li, Jiang, Shi, Bligh, et al., 2014), an arabinoglucan (Song et al., 2020), glucans (Gao, Bi, et al., 2010; Li, Jiang, Shi, Su, et al., 2014; Zhao et al., 2006), and glucomannan (Zhang et al., 2017). Comparatively, this study could be the first one giving clear evidence of the presence of pectin with HG backbone and RG-I domains in *Aconitum* plants. The roots and other plant parts of *A. carmichaelii* will be further explored for the presence of bioactive polysaccharides.

3.5. Complement fixation of polysaccharides from A. carmichaelii leaves

The complement fixation assay has been shown to be a good indicator for effects in the immune system by plant polysaccharides (Inngjerdingen et al., 2012; Zaitseva et al., 2020). As can be seen from Table 5, all isolated polysaccharide fractions from *A. carmichaelii* leaves except AL-I-II showed strong human complement fixating activities *in vitro*, and have higher activities than the positive control BP-II. The acidic fraction AL-I and one of its purified fractions, AL-I-I, were shown to be more potent than the neutral fraction AL-N ($p < 0.05$).

Complement fixating activity observed in the hemolysis assay could include activation and/or inhibition of the complement system, and these modulatory effects are related to structural difference of polysaccharides (Yamada & Kiyohara, 2007). Pectins with high *Mw* tend to be more active in the complement fixating assay (Togola et al., 2008; Zou et al., 2017). AL-I-I with a *Mw* of 169.1 kDa (Table 1) was shown to be more active than AL-I-II, which had a 4-fold lower *Mw* (41.6 kDa) and was found to be inactive. AL-N with an even lower *Mw*, on the other hand, did not follow this trend and was determined to be effective in complement fixation. This is most likely due to the various types of monosaccharide linkages. Effects of glucomannans on the complement system have not been much studied previously, but have shown to be inactive, except for highly heterogenous glucomannans mostly composed of 1,4-linked Glc, in addition to 1,3-linked Gal, 1,3-linked Fuc, 1,3-linked Man, and 1,3- or 1,6-linked Glc (Yamada & Kiyohara, 1999). As shown in Tables 2, 22.8 mol% of 1,4-linkded Glc, and minor amounts of 1,3-linked Gal (2.4 mol%) and 1,3-linked Glc (2.3 mol%) were all detected in AL-N. A comparable neutral polysaccharide primarily composed of Glc and Man from the African mushroom *Podaxon aegyptiacus* was reported with efficacy in the complement fixation assay as well (Diallo et al., 2002). In addition, the RG-I region in pectin has been reported to have high complement fixating activities, whereas the oligogalacturonides (HG domain) have weaker or negligible activities. Most arabinogalactans acting on the complement system are characterized as AG-II (Ferreira et al., 2015; Yamada & Kiyohara, 2007). These structure-activity relationships consequently explain the strongest complement fixating effect of AL-I-I among these fractions. Furthermore, an α-3,5-arabinofuranan have also demonstrated moderate complementary fixation in earlier studies (Yamada & Kiyohara, 2007), which is consistent with the current results that the active AL-I-I contains 1 mol% more 1,3,5-linked Ara units than the inactive AL-I-II, and partially explains the activity of AL-N which contained 2.6 mol% of 1,3,5-linked Ara units. Thus, AL-N and the branched pectic polysaccharide AL-I-I from *A. carmichaelii* leaves were found to have complement fixating activities and might be potential immunomodulatory substances.

Table 5
The inhibition of serum-induced hemolysis of sheep erythrocytes by polysaccharides from *Aconitum carmichaelii* leaves.

Sample name	ICH_{50} μg/mL
AL-N	18.3 ± 9.0^{b}
AL-I	8.1 ± 0.7^{a}
AL-I-I	6.6 ± 1.7^{a}
AL-I-II	>500
BP-II (positive control)	50.8 ± 3.6^{c}

Note: The different superscripted letters mean the statistical differences with $p < 0.05$ after Duncan's test.

3.6. Anti-inflammatory effects of polysaccharides from A. carmichaelii leaves on LPS-treated IPEC-J2 cells

All samples including AL-N, AL-I, AL-I-I and AL-I-II were tested for anti-inflammatory activities. As shown in Fig. 5A, cell viability of IPEC-J2 cells was not affected by 20 μg/mL of LPS treatment, but an inflammatory injury was caused by LPS according to the statistical upregulation of mRNA transcription of pro-inflammatory cytokines IL-1β, IL-6 and TNF-α (Fig. 5B, $p < 0.05$). Cell viability of cells co-cultivated with AL-N, AL-I-I or AL-I-II were shown to increase significantly ($p < 0.001$) compared with untreated cells (negative control), as shown in Fig. 5A. It was manifested that the possible glucomannan and pectic polysaccharides had no cytotoxic effect on IPEC-J2 cells, and could affect the proliferation of intestinal epithelial cells, as previously concluded by Huang et al. (2017). All polysaccharide fractions at a final concentration of 20 μg/mL were shown to inhibit the LPS-promoted gene expression of pro-inflammatory cytokines on IPEC-J2 cells at transcription level, including IL-1β, IL-6, and TNF-α (Fig. 5B). There was no statistically difference among the different fractions except that AL-N exerted a more potent effect in the inhibition of gene expression of IL-1β. AL-N is the first reported polysaccharide mainly consisting of mannans in *A. carmichaelii*. Its anti-inflammatory activity might be achieved through a direct contact with a cell surface mannose receptor, or mannose-binding lectins to prompt inflammatory response through cytokine expressions, as has been illustrated for most natural mannans (Tiwari et al., 2020). However, the rather low yield of AL-N compared to the high yield of AL-I resulted in the end of further in-depth biological studies of AL-N. Consequently, AL-I, and its purified fractions, AL-I-I and AL-I-II, were chosen as the main substances for further intestinal anti-inflammatory studies, which is also conductive to understand their effects in a microbiota-independent way.

As exhibited in Fig. 5C to F, the inflammatory injury caused by LPS was finally mitigated by all pectic polysaccharides in a light dose-dependent manner, by down-regulating mRNA transcriptions of pro-inflammatory cytokines IL-1β, IL-6, TNF-α and IL-18 ($p < 0.001$). AL-I led to a decrease in expression of IL-1β and IL-6, and a moderate suppression of the relative expressions of TNF-α and IL-18. The purified fractions AL-I-I and AL-I-II acted effectively on the inhibition of all inflammatory markers ($p < 0.05$), and no significant difference between AL-I-I and AL-I-II ($p > 0.05$) was observed, except a considerably higher efficacy of AL-I-II in reducing IL-6 expression ($p < 0.05$, Fig. 5D). The involvement of inflammatory pattern recognition receptors (PRR) was studied in order to further investigate the underlying mechanism of their anti-inflammatory effects. mRNA expressions of nucleotide-binding and oligomerization domain (NOD)-like receptor 1 (NOD1), NOD2, and TLR4 were upregulated by LPS, as shown in Fig. 5G, H, I. They were attenuated in all treated groups except NOD2, and a significant improvement was manifested in cells treated with AL-I-II compared with AL-I or AL-I-I ($p < 0.05$). Hence, the current study suggest that the pectic polysaccharides from *A. carmichaelii* leaves, AL-I-I and AL-I-II, possess promising anti-inflammatory activities on intestinal epithelial cells by inhibiting the expression of NOD1 and TLR4, but not by regulating NOD2. Further studies would be needed to determine how these pectic polysaccharides control the downstream proteins in TLR4 and NOD1 signal pathways using western-blot, and cells with depletion or silencing of TLR4 or NOD1would be included to confirm the regulatory effects at the same time. It is also of interest to investigate how AL-I-II exerted anti-inflammatory effects and through which receptor it works. The current results uncovered a promising medicinal use of these leaves in the treatment of intestinal inflammatory disease.

Similar effects of pectin consisting of a HG backbone with various

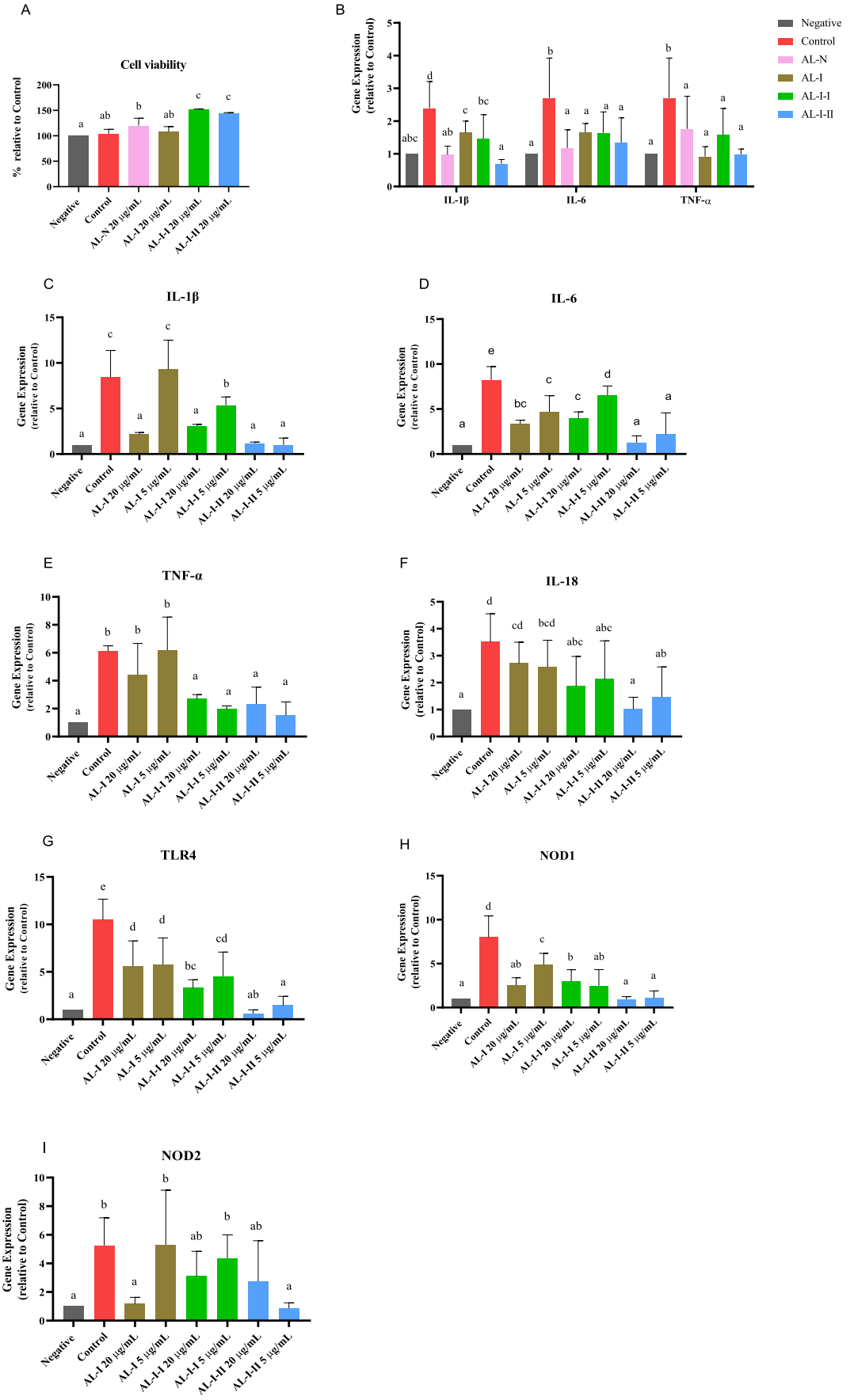

(caption on next page)

Fig. 5. Cell viability and anti-inflammatory effects of polysaccharides from *A. carmichaelii* leaves on IPEC-J2 cells. Cells were pre-treated with LPS for 12 h and then supplemented with samples at the final concentration of 20 and 5 μg/mL for a further 12 h. (A) Cell viability of cells after 12 h of co-culture determined by CCK-8. (B) Relative mRNA expressions of pro-inflammatory cytokines IL-1β, IL-6, and TNF-α after the treatment of AL-N, AL-I-I and AL-I-II at final concentration of 20 μg/mL quantified by qRT-PCR. Relative mRNA of pro-inflammatory cytokines IL-1β (C), IL-6 (D), TNF-α (E), and IL-18 (F), as well as inflammation-related receptors TLR4 (G), NOD1 (H), and NOD2 (I) were quantified by qRT-PCR. All values are presented as the means ± SD (n = 3). The different lowercase letters (a, b, c and d) labeled above the column indicate that the mean values are significantly different among groups in each plot ($p < 0.05$) according to the Duncan's multiple range test, but those columns labeled with the same lowercase letter are not ($p > 0.05$).

amounts of RG-I core chain, and neutral side chains have been reported previously (Wu et al., 2021; Zou et al., 2020; Zou et al., 2021). Specific relationships between pectin structures and immune responses on dendritic or macrophage cells have been demonstrated, and the degree of methylation, acetylation, RG-I, and RG-II of pectin are all crucial for anti-inflammatory properties on the immune barrier *via* immune cells, mucus layer, or PRRs (Beukema et al., 2020; Wu et al., 2021; Yang et al., 2022). Moreover, pectin has been highly reported to act indirectly on the intestinal immune system after being fermented in the colon, and chemical differences, like the degree of methylation, acetylation, and branch conditions would affect their activities (Wu et al., 2021). However, *in vitro* assays to determine the direct impact of pectin on intestinal epithelium in spite of bacteria, are not extensively studied, as well as the corresponding structure-activity relations. In the current study, both AL-I-I and AL-I-II performed similarly in most of the inhibitory effects of intestinal inflammation, but AL-I-II containing a longer HG backbone, β-Gal*p*A (Shen et al., 2021; Zhang, Li, et al., 2020), and terminal Rha*p* regions, was more potent. It is unclear whether these structural domains are dominant on anti-inflammatory effects compared to typical pectin with 1,4-linked α-Gal*p*A and RG-I domains. A further comprehensive evaluation of pectin with unexplored regions is still required. Moreover, the structure-activity relationship of different polysaccharides varies with the biological evaluation system. In the complement fixation assay, the linear AL-I-II with minor amounts of side chains were shown to be inactive, whereas it had potent anti-inflammatory activities. More comparative studies on the bioactivities of polysaccharides on multiple evaluations systems are needed to expand the structure-activity relationships of natural polysaccharides.

4. Conclusion

In the current study, a neutral polysaccharide fraction, AL-N, and two purified acidic polysaccharides fractions, AL-I-I and AL-I-II, were isolated and characterized. AL-N is possibly a fraction of heteromannans, mainly consisting of 1,4-linked Man*p* and 1,4-linked Glc*p*, in addition to a xyloglucan. AL-I-I and AL-I-II are pectic polysaccharides. AL-I-I is highly branched with RG-I regions containing arabinans, AG-II, and minor amounts of AG-I side chains, while, AL-I-II contains predominantly a linear HG backbone, with few side chains. All neutral and pectic polysaccharides from *A. carmichaelii* leaves were shown to have potent complement fixating activity. They also exerted intestinal anti-inflammatory effects on IPEC-J2 cells, and the high-yield pectins AL-I-I and AL-I-II were further shown to act through inhibiting expression of TLR4 and NOD1. This study presents a comprehensive chemical characterization of polysaccharides from *A. carmichaelii* leaves, and unravels their promising medicinal use as natural immunomodulatory and anti-inflammatory substances. Further, the use of this plant part would lead to less waste of biomaterial in the industrial processing of *A. carmichaelii* roots.

CRediT authorship contribution statement

Yu-Ping Fu: Data curation, Investigation, Methodology, Visualization, Roles/Writing - original draft. **Cen-Yu Li**: Data curation, Investigation, Methodology, Visualization. **Xi-Peng**: Data curation, Software. **Yuan-Feng Zou**: Funding acquisition, Methodology, Project administration, Resources, Supervision, Writing - review & editing. **Frode Rise**: Funding acquisition, Methodology. **Berit Smestad Paulsen**: Project administration, Writing - review & editing. **Helle Wangensteen**: Project administration, Supervision, Writing - review & editing. **Kari Tvete Inngjerdingen**: Methodology, Project administration, Supervision, Writing - review & editing.

Declaration of competing interest

The authors declare that they have no known competing financial interests or personal relationships that could have appeared to influence the work reported in this paper.

Acknowledgement

The first author acknowledges the funding from the China Scholarship Council (201906910066) and Sichuan Veterinary Medicine and Drug Innovation Group of China Agricultural Research System (SCCXTD-2020-18), and partly supported by the Research Council of Norway through the Norwegian NMR Platform, NNP (226244/F50). We acknowledge the support by the Key Laboratory of Animal Disease and Human Health of Sichuan Province, and help from Suthajini Yogarajah and Anne Grethe Hamre for methylation and GC–MS determination.

Appendix A. Supplementary data

Supplementary data to this article can be found online at https://doi.org/10.1016/j.carbpol.2022.119655.

References

Beukema, M., Faas, M. M., & de Vos, P. (2020). The effects of different dietary fiber pectin structures on the gastrointestinal immune barrier: Impact via gut microbiota and direct effects on immune cells. *Experimental and Molecular Medicine, 52*, 1364–1376.

Bradford, M. M. (1976). A rapid and sensitive method for the quantitation of microgram quantities of protein utilizing the principle of protein-dye binding. *Analytical Chemistry, 72*(1–2), 248–254.

Braünlich, P. M., Inngjerdingen, K. T., Inngjerdingen, M., Johnson, Q., Paulsen, B. S., & Mabusela, W. (2018). Polysaccharides from the South African medicinal plant Artemisia afra: Structure and activity studies. *Fitoterapia, 124*, 182–187.

Chambers, R. E., & Clamp, J. R. (1971). An assessment of methanolysis and other factors used in the analysis of carbohydrate-containing materials. *Biochemical Journal, 125*, 1009–1018.

Chen, H. (2011). Components analysis of volatile oil from different tissues of Aconitum carmichaeli Debx. *Journal of Anhui AgriculturalScience, 39*(6), 3325–3326, 3367.

China Academy of Chinese Medical Science, Chinese Medicine Research Center. (2017). Dynamic detection of Traditional Chinese Medicine resources. http://zyzyjc.zyzypc.com.cn/page/monitor.html. (Accessed 22 January 2021).

Chinese Pharmacopoeia Committee. (2020). *Chinese Pharmacopoeia* (2020 ed.). Beijing: Chemical Industry Press.

Ciucanu, I., & Kerek, F. (1984). A simple and rapid method for the permethylation of carbohydrates. *Carbohydrate Research, 131*(2), 209–217.

Committee for the flora of China, Chinese Academy of Science. (2004). *Flora of China.* Beijing: Science Press.

Cui, S. W., Phillips, G. O., Blackwell, B., & Nikiforukc, J. (2007). Characterisation and properties of Acacia senegal (L.) Willd. var. senegal with enhanced properties (Acacia (sen) SUPERGUMTM): Part 4. Spectroscopic characterisation of Acacia senegal var. senegal and Acacia (sen) SUPERGUMTM arabic. *Food Hydrocolloids, 21*, 347–352.

Diallo, D., Sogn, C., Samaké, F. B., Paulsen, B. S., Michaelsen, T. E., & Keita, A. (2002). Wound healing plants in Mali the Bamako region, an ethnobotanical survey and complement fixation of water extracts from selected plants. *Pharmaceutical Biology, 40*(2), 117–128.

Dubois, M., Gilles, K. A., Hamilton, J. K., Rebers, P. A., & Smith, F. (1956). Colorimetric method for determination of sugars and related substances. *Analytical Chemistry, 28*(3), 350–356.

Duc, L. V., Thanh, T. B., Thanh, H. N., & Tien, V. N. (2015). Flavonoids and other compound isolated from leaves of Aconitum carmichaelii Debx. growing in Viet Nam. *Journal of Chemical and Pharmaceutical Research, 7*(6), 228–234.
Ferreira, S. S., Passos, C. P., Madureira, P., Vilanova, M., & Coimbra, M. A. (2015). Structure–function relationships of immunostimulatory polysaccharides: A review. *Carbohydrate Polymers, 132*, 378–396.
Fry, S. C. (2011). Cell wall polysaccharide composition and covalent crosslinking. *Annual Plant Reviews, 41*, 1–42.
Fry, S. C., York, W. S., Albersheim, P., Darvill, A., Hayashi, T., Joseleau, J.-P., Kato, Y., Lorences, E. P., Maclachlan, G. A., McNeil, M., Mort, A. J., Reid, J. S. G., Seitz, H. U., Selvendran, R. R., Voragen, A. G. J., & White, A. R. (1993). An unambiguous nomenclature for xyloglucan-derived oligosaccharides. *Physiologia Plantarum, 89*(1), 1–3.
Fu, Y.-P., Zou, Y.-F., Lei, F.-Y., Wangensteen, H., & Inngjerdingen, K. T. (2022). Aconitum carmichaelii Debeaux: A systematic review on traditional use, and the chemical structures and pharmacological properties of polysaccharides and phenolic compounds in the roots. *Journal of Ethnopharmacology, 291*, Article 115148.
Gao, T., Bi, H., Ma, S., & Lu, J. (2010). Structure elucidation and antioxidant activity of a novel α- (1→3), (1→4)-D-glucan from Aconitum kusnezoffii Reichb. *International Journal of Biological Macromolecules, 46*, 85–90.
Gao, T., Bia, H., Ma, S., & Lu, J. (2010). The antitumor and immunostimulating activities of water soluble polysaccharides from Radix aconiti, Radix aconiti lateralis and Radix aconiti kusnezoffii. *Natural Product Communications, 5*(3), 447–455.
Grønhaug, T. E., Kiyohara, H., Sveaass, A., Diallo, D., Yamada, H., & Paulsen, B. S. (2011). Beta-D-(1–4)-galactan-containing side chains in RG-I regions of pectic polysaccharides from Biophytum petersianum Klotzsch. Contribute to expression of immunomodulating activity against intestinal Peyer's patch cells and macrophages. *Phytochemistry, 72*, 2139–2147.
Guo, D. (2012). *Studies on chemical constituents of raw slices of Aconitum carmichaelii Debx*. Chengdu, China: Chengdu University of TCM. Master's Degree.
Hayashi, T., & Kaida, R. (2011). Functions of xyloglucan in plant cells. *Molecular Plant, 4*, 17–24.
He, Y.-N., Ou, S.-P., Xiong, X., Pan, Y., Pei, J., Xu, R.-C., Geng, F.-N., Han, L., Zhang, D.-K., & Yang, M. (2018). Stems and leaves of Aconitum carmichaelii Debx. as potential herbal resources for treating rheumatoid arthritis: Chemical analysis, toxicity and activity evaluation. *Chinese Journal of Natural Medicines, 16*(9), 644–652.
Huang, C., Li, Z. X., Wu, Y., Huang, Z. Y., Hu, Y., & Gao, J. (2021). Treatment and bioresources utilization of traditional Chinese medicinal herb residues: Recent technological advances and industrial prospect. *Journal of Environmental Management, 299*, Article 113607.
Huang, C., Peng, X., Pang, D.-J., Li, J., Paulsen, B. S., Rise, F., Chen, Y.-L., Chen, Z.-L., Jia, R.-Y., Li, L.-X., Song, X., Feng, B., Yin, Z.-Q., & Zou, Y.-F. (2021). Pectic polysaccharide from Nelumbo nucifera leaves promotes intestinal antioxidant defense in vitro and in vivo. *Food & Function, 12*, 10828.
Huang, X., Nie, S., & Xie, M. (2017). Interaction between gut immunity and polysaccharides. *Critical Reviews in Food Science and Nutrition, 57*(14), 2943–2955.
Inngjerdingen, K. T., Meskini, S., Austarheim, I., Ballo, N., Inngjerdingen, M., Michaelsen, T. E., Diallo, D., & Paulsen, B. S. (2012). Chemical and biological characterization of polysaccharides from wild and cultivated roots of Vernonia kotschyana. *Journal of Ethnopharmacology, 139*, 350–358.
Kaczmarska, A., Pieczywek, P. M., Cybulska, J., & Zdunek, A. (2022). Structure and functionality of Rhamnogalacturonan I in the cell wall and in solution: A review. *Carbohydrate Polymers, 278*, Article 118909.
Kostálová, Z., Hromádková, Z., & Ebringerová, A. (2013). Structural diversity of pectins isolated from the Styrian oil-pumpkin (Cucurbita pepo var. styriaca) fruit. *Carbohydrate Polymers, 93*, 163–171.
Li, X., Jiang, J., Shi, S., Bligh, S. W. A., Li, Y., Jiang, Y., Huang, D., Ke, Y., & Wang, S. (2014). A RG-II type polysaccharide purified from Aconitum coreanum alleviates lipopolysaccharide-induced inflammation by inhibiting the NF-kB signal pathway. *Plos One, 9*(6), Article e99697.
Li, X., Jiang, J., Shi, S., Su, Y., Jiang, Y., Ke, Y., & Wang, S. (2014). Anti-complementary activities of a (1→6) linked glucan from korean mondshood root and its sulfated derivatives. *Chemical Journal of Chinese Universities, 35*(7), 1423–1426.
Makarova, E. N., Shakhmatov, E. G., & Belyy, V. A. (2016). Structural characteristics of oxalate-soluble polysaccharides of Sosnowsky's hogweed (Heracleum sosnowskyi Manden). *Carbohydrate Polymers, 153*, 66–77.
Michaelsen, T. E., Gilje, A., Samuelsen, A. B., Høgåsen, K., & Paulsen, B. S. (2000). Interaction between human complement and a pectin type polysaccharide fraction, PM II, from the leaves of Plantago major L. *Scandinavian Journal of Immunology, 52*, 483–490.
Ni, S., Pan, Y., Zou, J., Fu, C., & Wu, P. (2002). The study of chemical volatile oils of Aconitum carmichaelii Debx. by GC-MS. *Chinese Traditional and Herbal Drugs, 33*(8), 691–692.
Nishinari, K., Takemasa, M., Zhang, H., & Takahashi, R. (2007). Storage plant polysaccharides: Xyloglucans, galactomannans, glucomannans. In H. Kamerling (Ed.), *Comprehensive glycoscience* (pp. 613–652). Elsevier Oxford.
Ou, S., Wang, S., Zheng, Q., Hu, P., Chen, Z., & Yang, M. (2013). Investigation of dynamic differences of crude polysaccharides content in various tissues of Aconitum carmichaelii. *Chinese Journal of Experimental Traditional Medical Formulae, 19*(5), 7–9.
Patova, O. A., Luanda, A., Paderin, N. M., Popov, S. V., Makangara, J. J., Kuznetsov, S. P., & Kalmykova, E. N. (2021). Xylogalacturonan-enriched pectin from the fruit pulp of Adansonia digitata: Structural characterization and antidepressant-like effect. *Carbohydrate Polymers, 262*, Article 117946.
Patova, O. A., Smirnov, V. V., Golovchenko, V. V., Vityazev, F. V., Shashkov, A. S., & Popov, S. V. (2019). Structural, rheological and antioxidant properties of pectins from Equisetum arvense L. and Equisetum sylvaticum L. *Carbohydrate Polymers, 209*, 239–249.
Pettolino, F. A., Walsh, C., Fincher, G. B., & Bacic, A. (2012). Determining the polysaccharide composition of plant cell walls. *Natural Protocol, 7*(9), 1590–1607.
Rosenbohm, C., Lundt, I., Christensen, T. I. E., & Young, N. G. (2003). Chemically methylated and reduced pectins: Preparation, characterisation by 1H NMR spectroscopy, enzymatic degradation, and gelling properties. *Carbohydrate Research, 338*(7), 637–649.
Saha, A., & Basak, B. B. (2020). Scope of value addition and utilization of residual biomass from medicinal and aromatic plants. *Industrial Crops and Products, 145*, Article 111979.
Shakhmatov, E. G., Atukmaev, K. V., & Makarova, E. N. (2016). Structural characteristics of pectic polysaccharides and arabinogalactan proteins from Heracleum sosnowskyi Manden. *Carbohydrate Polymers, 136*, 1358–1369.
Shakhmatov, E. G., Belyy, V. A., & Makarova, E. N. (2018). Structure of acid-extractable polysaccharides of tree greenery of Picea abies. *Carbohydrate Polymers, 199*, 320–330.
Shakhmatov, E. G., Makarova, E. N., & Belyy, V. A. (2019). Structural studies of biologically active pectin-containing polysaccharides of pomegranate Punica granatum. *International Journal of Biological Macromolecules, 122*, 29–36.
Shakhmatov, E. G., Udoratina, E. V., Atukmaev, K. V., & Makarova, E. N. (2015). Extraction and structural characteristics of pectic polysaccharides from Abies sibirica L. *Carbohydrate Polymers, 123*, 228–236.
Shen, Y., Liang, J., Guo, Y. L., Li, Y., Kuang, H. X., & Xia, Y. G. (2021). Ultrafiltration isolation, structures and anti-tumor potentials of two arabinose- and galactose-rich pectins from leaves of Aralia elata. *Carbohydrate Polymers, 255*, Article 117326.
Singleton, V. L., & Rossi, J. A. (1965). Colorimetry of total phenolics with phosphomolybdic-phosphotungstic acid reagent. *American Journal of Enology and Viticulture, 16*, 144–158.
Song, J., Wu, Y., Ma, X., Feng, L., Wang, Z., Jiang, G., & Tong, H. (2020). Structural characterization and α-glycosidase inhibitory activity of a novel polysaccharide fraction from Aconitum coreanum. *Carbohydrate Polymers, 230*, Article 115586.
Sweet, D. P., Shapiro, R. H., & Albersheim, P. (1975). Quantitative analysis by various g. l.c. response-factor theories for partially methylated and partially ethylated alditol acetates. *Carbohydrate Research, 40*(2), 217–225.
Tang, C., Ding, R., Sun, J., Liu, J., Kan, J., & Jin, C. (2019). The impacts of natural polysaccharides on intestinal microbiota and immune responses -A review. *Food & Function, 10*, 2290.
Tiwari, U. P., Fleming, S. A., Abdul Rasheed, M. S., Jha, R., & Dilger, R. N. (2020). The role of oligosaccharides and polysaccharides of xylan and mannan in gut health of monogastric animals. *Journal of Nutritional Science, 9*, Article e21.
Togola, A., Inngjerdingen, M., Diallo, D., Barsett, H., Rolstad, B., Michaelsen, T. E., & Paulsen, B. S. (2008). Polysaccharides with complement fixing and macrophage stimulation activity from Opilia celtidifolia, isolation and partial characterisation. *Journal of Ethnopharmacology, 115*, 423–431.
Varki, A., Cummings, R. D., Aebi, M., Packer, N. H., Seeberger, P. H., Esko, J. D., Stanley, P., Hart, G., Darvill, A., Kinoshita, T., Prestegard, J. J., Schnaar, R. L., Freeze, H. H., Marth, J. D., Bertozzi, C. R., Etzler, M. E., Frank, M., Vliegenthart, J. F., Lütteke, T., … Kornfeld, S. (2015). Symbol nomenclature for graphical representations of glycans. *Glycobiology, 25*(12), 1323–1324.
Voragen, A. G. J., Coenen, G.-J., Verhoef, R. P., & Schols, H. A. (2009). Pectin, a versatile polysaccharide present in plant cell walls. *Structural Chemistry, 20*(2), 263–275.
Wang, B. B., Wang, J. L., Yuan, J., Quan, Q. H., Ji, R. F., Tan, P., Han, J., & Liu, Y. G. (2016). Sugar composition analysis of fuzi polysaccharides by HPLC-MS(n) and their protective effects on Schwann cells exposed to high glucose. *Molecules, 21*(11), 1496.
Wang, X., Zhao, X., Lv, Y., Hu, M., Fan, L., Li, Q., Cai, C., Li, G., & Yu, G. (2019). Extraction, isolation and structural characterization of a novel polysaccharide from Cyclocarya paliurus. *International Journal of Biological Macromolecules, 132*, 864–870.
Wold, C. W., Kjeldsen, C., Corthay, A., Rise, F., Christensend, B. E., Duusb, J.Ø., & Inngjerdingen, K. T. (2018). Structural characterization of bioactive heteropolysaccharides from the medicinal fungus Inonotus obliquus (Chaga). *Carbohydrate Polymers, 185*, 27–40.
Wu, D., Yu, C., & Chen, S. (2021). Dietary pectic substances enhance gut health by its polycomponent: A review. *Comprehensive Reviews in Food Science and Food Safety, 20*, 2015–2039.
Yamada, H., & Kiyohara, H. (1999). Complement-activating polysaccharides from medicinal herbs. In H. Wagner (Ed.), *Immunomodulatory agents from plants* (pp. 161–202). Basel: Birkhäuser.
Yamada, H., & Kiyohara, H. (2007). Immunomodulating activity of plant polysaccharide structures. In H. Kamerling (Ed.), *Comprehensive glycoscience* (pp. 663–694). Oxford: Elsevier.
Yang, L., Zhao, N., Wang, J., Wang, X., & Liu, S. (2011). Chemical constituents of the aerial part of Aconitum carmichaelii Debx. *Anhui Medical and Pharmaceutical Journal, 15*(9), 1068–1069.
Yang, W., Zhao, P., Li, X., Guo, L., & Gao, W. (2022). The potential roles of natural plant polysaccharides in inflammatory bowel disease: A review. *Carbohydrate Polymers, 277*, Article 118821.
Yang, X., Wu, Y., Zhang, C., Fu, S., Zhang, J., & Fu, C. (2020). Extraction, structural characterization, and immunoregulatory effect of a polysaccharide fraction from Radix Aconiti Lateralis Preparata (Fuzi). *International Journal of Biological Macromolecules, 143*, 314–324.
Yao, H.-Y.-Y., Wang, J.-Q., Yin, J.-Y., Nie, S.-P., & Xie, M.-Y. (2021). A review of NMR analysis in polysaccharide structure and conformation: Progress, challenge and perspective. *Food Research International, 143*, Article 110290.

Yu, Y., Shen, M., Song, Q., & Xie, J. (2018). Biological activities and pharmaceutical applications of polysaccharide from natural resources: A review. *Carbohydrate Polymers, 183*, 91–101.

Zaitseva, O., Khudyakov, A., Sergushkina, M., Solomina, O., & Polezhaeva, T. (2020). Pectins as a universal medicine. *Fitoterapia, 146*, Article 104676.

Zhang, H., Li, C., Ding, J., Lai, P. F. H., Xia, Y., & Ai, L. (2020). Structural features and emulsifying stability of a highly branched arabinogalactan from immature peach (Prunus persica) exudates. *Food Hydrocolloids, 104*, Article 105721.

Zhang, L., Yang, C., Luo, Q., Liu, J., Chen, Y., & Yong, S. (2020). Non-diterpenoid alkaloids in aerial parts of Aconitum carmichaelii. *Chinese Traditional and Herbal Drugs, 51*(3), 588–593.

Zhang, S., He, F., Chen, X., & Ding, K. (2019). Isolation and structural characterization of a pectin from Lycium ruthenicum Murr and its anti-pancreatic ductal adenocarcinoma cell activity. *Carbohydrate Polymers, 223*, Article 115104.

Zhang, Y., Wu, W., Kang, L., Yu, D., & Liu, C. (2017). Effect of Aconitum coreanum polysaccharide and its sulphated derivative on the migration of human breast cancer MDA-MB-435s cell. *International Journal of Biological Macromolecules, 103*, 477–483.

Zhao, C., Li, M., Luo, Y., & Wu, W. (2006). Isolation and structural characterization of an immunostimulating polysaccharide from fuzi,Aconitum carmichaeli. *Carbohydrate Research, 341*(4), 485–491.

Zou, Y.-F., Chen, M., Fu, Y.-P., Zhu, Z.-K., Zhang, Y.-Y., Paulsen, B. S., Rise, F., Chen, Y.-L., Yang, Y.-Z., Jia, R.-Y., Li, L.-X., Song, X., Tang, H.-Q., Feng, B., Lv, C., Ye, G., Wu, D.-T., Yin, Z.-Q., & Huang, C. (2021). Characterization of an antioxidant pectic polysaccharide from Platycodon grandiflorus. *International Journal of Biological Macromolecules, 175*, 473–480.

Zou, Y.-F., Fu, Y.-P., Chen, X.-F., Austarheim, I., Inngjerdingen, K. T., Huang, C., Lei, F.-Y., Song, X., Li, L., Ye, G., Eticha, L. D., Yin, Z., & Paulsen, B. S. (2017). Polysaccharides with immunomodulating activity from roots of Gentiana crassicaulis. *Carbohydrate Polymers, 172*, 306–314.

Zou, Y.-F., Zhang, Y.-Y., Paulsen, B. S., Rise, F., Chen, Z.-L., Jia, R.-Y., Li, L.-X., Song, X., Feng, B., Tang, H.-Q., Huang, C., Yea, G., & Yin, Z.-Q. (2020). New pectic polysaccharides from Codonopsis pilosula and Codonopsis tangshen: Structural characterization and cellular antioxidant activities. *Journal of the Science of Food and Agriculture, 101*(14), 6043–6052.